The influence of hydrography on pelagic fish distribution and communities in a sub-arctic estuary (Lake Melville, Labrador)

By

©Tiffany Small

A thesis submitted to the School of Graduate Studies in partial fulfillment of the requirements for the degree of Master of Science in Fisheries Science and Technology

Fisheries and Marine Institute
Center for Fisheries Ecosystem Research
Memorial University of Newfoundland and Labrador

May 2023
St. John's, Newfoundland and Labrador

Acknowledgements

The high degree of collaboration that led to this master's thesis is a testament to the interdisciplinary nature of ecological research as well as the importance of incorporating different perspectives to one research question. Though this thesis is my own, I would not have been able to produce this research without the help of many individuals in both my professional and personal life. I am extremely grateful for all the learning opportunities I have gained from this process, and I can honestly say that the connections I've made throughout the past four years will continue to prosper after this chapter ends. I want to personally thank everyone who had a hand working with my project. To start, I would like to thank my supervisor Dr. Maxime Geoffroy for trusting me, teaching me, and allowing me to learn from my mistakes. I am forever grateful for your patience and understanding as COVID-19 required us to pivot numerous times all the while I was navigating quite literally the most challenging chapter of my adult life so far. I deeply appreciate our ability to work together given our different academic backgrounds and will always remember our numerous games of trivia in the field. Thank you to my committee member, Dr. James McCarthy for helping steer the objectives of this project in its early stages and for providing many edits (even while travelling during a snowstorm!). I am very grateful for your perspective and how your expertise has improved the quality of this project. I would also like to thank Dr. Marie Clément for initiating the collaborations and field work on which this thesis is based. It was because of her years of experience working in the area that we were able to connect with the land and the people and appreciate Nunatsiavut landscape in all its glory. Many thanks go out to Doug Blake for guiding and sharing his expertise in the field (especially while putting up with all the times I said I was cold). A huge thank you to Adam Templeton for helping with the mooring and providing technical expertise for the majority of this project.

When I wasn't in Labrador for field work, I was counting plankton or sifting through Rainbow smelt stomachs in the lab (before the pandemic). I am very thankful to Jessica Randall who, despite being exceptionally busy with her own master's research, took the time to walk me through sampling protocols and for spending countless hours answering my questions and listening to my hardships. A huge thank you to my pals in the Geoffroy lab for the constant motivation and support even when none of us knew what we were doing, I am so proud of everyone's tenacity moving through graduate school in the middle of a pandemic. Whether it was from Newfoundland or Norway, we still managed to focus, strategize, and commit to get the job done.

Thank you to the Marine Environmental Observation, Prediction and Response Network (MEOPAR) for providing financial support as well as the numerous networking and professional development opportunities to collaborate with colleagues across Canada and beyond. I am grateful to have studied at the Marine Institute of Memorial University of Newfoundland (MI) as the tightly knit academic community really made St. John's feel like home throughout this graduate degree.

I could not have made it to the finish line without the support of my family and friends. Thank you to my parents for always believing in me, even when I did not believe in myself. Thank you to my best friends and MI family for reminding me to take breaks and providing balance through endless laughs and craft beer. A huge thank you to my grandmother, Lillian Small, who would spend countless hours with me as a child beach combing and splashing around in tide pools. I seriously would not be here without you, Nan. Finally, I am the most grateful for the support of my partner,

Logan. You have demonstrated so much patience, kindness, and encouragement throughout this process despite spending half of it in a different province. I will forever be thankful for your constant love and support and keeping me from completely losing my marbles. Thank you.

Table of Contents

Acknowledgements ***2***

List of Figures ***7***

List of Tables ***9***

Co-authorship Statement ***10***

Thesis structure **11**

General Abstract ***12***

Chapter 1: General Introduction ***13***

1.1.1. Estuaries and estuarine circulation 13
1.1.2. Fjord estuaries 15
1.1.3. Habitat use in estuaries and biodiversity 17
1.1.4. The Lake Melville Estuary 20
1.1.5. Fish community in Lake Melville 22
1.1.6. The role of sentinel species 24

Methods for monitoring estuarine ecosystems **26**

1.2.1. Hydroacoustics 26
1.2.2. Spatial analysis 30
1.2.3. Ground truthing and environmental DNA 31

Rationale and research objectives ***33***

Chapter 2: Strong water stratification drives the distribution of pelagic fish in a sub-arctic estuary (Lake Melville, Labrador) ***34***

Abstract **34**

Introduction **35**

Methods **37**

2.3.1. Study area 37
2.3.2. Survey design 38
2.3.3. Environmental data 39
2.3.4. Acoustics 40
2.3.5. Fish sampling 42
2.3.6. Environmental DNA 43

Results **45**

2.4.1. Environmental parameters 45
2.4.2. Vertical and spatial distribution of pelagic fish 48
2.4.3. Biodiversity of pelagic fish 50
2.4.5. Environmental DNA 50

Discussion **51**

4.1 The low salinity surface layer and pycnocline of Lake Melville as a habitat for rainbow smelt larvae 51
4.2 Fish diversity and distribution 54
4.3 Assessing the impact of further river harnessing 56
4.4 Conclusions 57

Chapter 3: General Conclusions ***58***

References ***61***

Figures ***71***

Tables ***84***

Appendix ***90***

Supplementary material 90

List of Figures

Figure 1. Stratification-circulation diagram from Hansen and Rattray (1996). Fraction of horizontal salt balance by diffusion, $\delta SS0$ represents the stratification parameter and $UsUf$ represents the circulation parameter. When the diffusive fraction (ν) equals 1, gravitational convection ceases, and diffusion is entirely responsible for the upstream salt flux. As $\nu \rightarrow 0$ diffusion becomes less significant, and the upstream salt flux is caused by gravitational convection. 71
Figure 2. Expanded applications based on Hansen and Rattray (1966) (Figure 1) of the adjusted and extended classification diagram based on the regimes of (Dijkstra and Schuttelaars 2020) taken from Dijkstra and Schuttelaars (2021). Estuaries are denoted by black dots, lines denote along-channel stretch of the estuary. The letters indicate: C: Columbia (United States), D: Delaware (United States), Du: Duwamish (United States), E: Ems (Germany), F: Fraser (Canada), H: Hudson (United States), J: James (United States) M: Mississippi (United States), NM: Mersey Narrows (United Kingdom), R: Rotterdam Waterway (branch of the Rhine-Meuse delta, Netherlands), Sc: Scheldt (Belgium, Netherlands), Sy: Strymon (Greece). Subscripts l, m, and h denote low, moderate, and high river discharge. Grey spaces indicated unpermitted or physically unrealistic solutions. 72
Figure 3. Map of Labrador from Durkalec et al. (2016) showing Nunatsiavut "Our Beautiful Land" and the Lake Melville System including the locations of the Churchill Falls Dam and Muskrat Falls Dam (yellow stars). 73
Figure 4. Schematic from MacLennan and Simmonds (2013) illustrating the acoustic energy propagating outwards from the transducer (size of 7°). (a) Spherical spreading showing that the intensity reduces as range increases. (b) This causes the intensity of the point source to follow the inverse-square law (curve 1). Near-field effect then limits the intensity close to the transducer face (curve 2). 74
Figure 5. Bathymetric map of upper Lake Melville. The continuous gray line indicates the acoustic transect followed in summers 2018 and 2019. Environmental stations (dots) were samples in summer and winter. The locations of fyke and gill net sampling are denoted by triangles (2018) and crosses (2019). The star indicates the position of the long-term oceanographic mooring. 75
Figure 6. Section plots of conservative temperature (θ) and absolute salinity (SA) during summers 2018 and 2019 and winters 2019 and 2020 across Goose Bay (GB; west) and Upper Lake Melville (ULM; east). For each panel, the density anomaly referenced to surface (σ0; in kg m-3) is plotted as solid light gray lines identified in the salinity panels. The brown shaded polygon represents bottom drawn using the depth at each station determined with acoustics measurements. The grey dotted lines represent profile stations identified in the top of the salinity panels. White areas indicate the absence of data. The pycnocline is identified with a dashed-red lines. The separation between Goose Bay (GB) and Upper Melville Lake (ULM) occurs at the sill near station 5 and is identified in the salinity panel. Note that for winter 2019, a problem with the profiler prevented the presentation of data below ~20m. 76
Figure 7. Turbidity (in Formazine Turbidity Unit; FTU) and chl-a (in part per billion; ppb) section plot for Goose Bay (GB) and Upper Lake Melville (ULM) during winter 2019. For each panel, the density anomaly referenced to surface (σ_0; in kg m^{-3}) is plotted as solid light gray lines

identified in the chl-a panel. The vertical dashed lines indicate the location of the stations. The sill between GB and ULM is identified in brown. 77
Figure 8. Temperature contours at the mooring location from two deployments (2019-07-15 to 2020-10-14 and 2020-10-13 to 2021-10-04), from 6 TidbiTs temperature sensors (position identified with dashed-gray lines), one RBR CTD located at 8m during the first deployment (dashed-blue line) and 38.4m during the second deployment (dashed-red line) and one Seabird CTD located at 11m during the second deployment (dashed-green line). Note that during the second deployment, the mooring release got tangled bringing all instruments down by about 3 m from their targeted depth. 78
Figure 9. Examples of raw SV echograms at 38 kHz at station 2 during A) summer 2018 as measured with a hull mounted Simrad EK60; and B) winter 2019 as measured with a Simrad Wideband Autonomous Transceiver (WBAT). The dashed red lines indicate the sound scattering layer, which in this case was located between 9 and 15 m. Corresponding temperature (red) and salinity (black) profiles for station 2 in C) summer 2018 and D) winter 2019. 79
Figure 10. Percentage of total Target Strengths (TS) at 38 kHz for A) pooled summer data (2018-2019; n=122,924); and B) pooled winter data (2019-2020; n=18,175) at depth □25 m (orange) and >25 m (gray). Average depth of each target and their corresponding TS for targets detected in C) summer and D) winter. The maximum range of the WBAT and portable echosounder in winter was set to only 100 m. 80
Figure 11. Percent total of Target Strength values of pooled results for summers 2018 and 2019, divided by regions (ULM (blue) and GB (red)). Showing TS distributions, A) ≤ 25 m and B) in depths greater than 25 m. 81
Figure 12. Kriged nautical area scattering strength (S_A in dB re $1m^2$ nmi^{-2}) at A) 38 kHz and B) 120 kHz above and below 25 m. The dashed line delineates Goose Bay (GB) and upper Lake Melville (ULM). 82
Figure 13. Nautical area scattering strength (S_A in dB re $1m^2$ nmi^{-2}) at 38 kHz above and below 25m. The dashed line delineates Goose Bay (GB) and upper Lake Melville (ULM). 83

List of Tables

Table 1. Average seasonal pycnocline depth, temperature, and salinity above (surface layer) and below (bottom waters) the pycnocline in Goose Bay and Upper Lake Melville. The information is divided into year 1 (2018-2019) and year 2 (2019-2020) of the survey. Standard variation is indicated. 84
Table 2. Mean abundance and biomass in fyke and gill nets..... 85
Table 3. Shannon-Weiner diversity Index (H) by region and year calculated from catches in gill and fyke nets deployed in shallow water (<2m). 86
Table 4 Environmental DNA hits above and below the pycnocline in Upper Lake Melville and Goose Bay divided based on species habitat (blue = Marine, grey = Freshwater, green = Anadromous)..... 87

Co-authorship Statement

I was responsible for most of the work in this thesis with the support of my supervisor Dr. Maxime Geoffroy and my colleague Jordan Sutton. This thesis investigates the relationship between estuarine stratification and pelagic fish abundance distribution and diversity. It also emphasizes the importance of long-term monitoring in Lake Melville and encourages the use of Rainbow smelt as a sentinel species to explore how changes in the seasonality of freshwater flow from hydroelectric dams impact estuarine ecosystems.

This thesis incorporates data that were collected in 2018 (1 year prior to my involvement as a master's in science student), 2019 and 2020. Drs. Marie Clément and Maxime Geoffroy engaged in field work in summer 2018 and winter 2019 with the support from the NunatuKavut Community Council, Nunatsiavut Government, and the Innu Nation. I was involved in field work on site in Labrador for summer 2019 and winter 2020, alongside Dr. Maxime Geoffroy and Jordan Sutton. I obtained gill and fyke net catch data collected by Matthew Gosse from WSP E&I Canada Ltd. from summer 2018 and 2019. Environmental DNA was collected in 2018 by Drs. Marie Clément and Maxime Geoffroy and analyzed by Dr. Louis Bernatchez's team from Université Laval. I cleaned, scrutinized, and analyzed all acoustic data with the help of Jordan Sutton. I conducted all the statistical analyses and manuscript preparation for this thesis with supporting comments from my committee.

Thesis structure

Chapter 1 of this thesis is a literature review structured as a general introduction to provide background on necessary contextual elements to support the main objectives of Chapter 2. Chapter 2 presents the core of the study and investigates the abundance, assemblage, and distribution of pelagic fish in relation to the stratification of Lake Melville. This chapter also delves into the use of Rainbow smelt as a sentinel species and the importance of long-term monitoring in estuaries affected by hydroelectric projects. This main chapter is to be submitted as a peer-reviewed paper to the journal of Estuarine, Coastal and Shelf Science. Chapter 3 is the general conclusion which wraps up the key findings of the research presented herein and offers recommendations to improve future ecological research involving estuaries.

General Abstract

Estuaries are semi-enclosed bodies of water that are influenced by freshwater runoff and saltwater from neighbouring oceans. Water masses in estuaries can be strongly stratified and are often influenced by geological, hydrological and hydrographical features. The stratification of the water column in estuaries creates important nursery habitats for larvae and juvenile fish populations. The Lake Melville system, a highly stratified sub-arctic estuary in Labrador, spans 2100 km^2 and is considered the longest single body of water in Labrador (250 km). By pairing seasonal hydroacoustic surveys conducted in summers 2018-2019 and winters 2019-2020 with ichthyoplankton and gill nets sampling as well as environmental DNA, we test the hypothesis that the strong water stratification prevailing in upper Lake Melville provides a refuge for early life stages of fish. We found that adult pelagic fish occupied the Atlantic waters below the steep pycnocline, while ichthyoplankton aggregated just above and within the pycnocline (as deep as 25 m). Nine species of fish were captured in gill and fyke nets and 53 fish species were detected with environmental DNA. Larvae of Rainbow smelt (*Osmerus mordax*) were ubiquitous in July and August and represented 100 % of the ichthyoplankton assemblage during these months. No fish larvae were caught in winter (February). As seen in other estuaries, we conclude that the layer of freshwater provides a refuge for Rainbow smelt larvae, a key forage species in the estuary. The recent completion of a large hydroelectric project on the main affluent of Lake Melville could alter the seasonal flow of freshwater and, ultimately, fish distribution. This study contributes to the growing library of resources from which to assess future changes in biodiversity and distribution of fish in the estuary.

Chapter 1: General Introduction

1.1.1. Estuaries and estuarine circulation

An estuary is a semi-enclosed coastal body of water, whereby water circulation occurs from the interaction between the less dense freshwater influx from rivers and the denser deep saline waters from neighbouring seas. A tidal prism is the volume of water in an estuary between mean high and mean low tide. Estuarine fluxes occurring near the open ocean are dependent on the estuary tidal prism and magnitude of freshwater run-off. The freshwater inputs are regulated by natural forces (i.e. rainfall, melting of snow and glaciers) and human freshwater management upstream (i.e. irrigation, flooding, water storage for electricity generation (Campuzano et al. 2017)). Understanding natural and anthropogenic variability in freshwater inputs to an estuary is critical when studying how hydrodynamics impact its ecosystem.

Historically, the classification of estuaries relied heavily on the degree of stratification, as suggested by Hansen and Rattray (1966). This classification used two primary salt import mechanisms: dispersion attributed to tides and vertical shear dispersion due to gravitational circulation, to discriminate between seven types of estuaries. The four most common types are Type 1: slightly stratified, Type 2: vertically mixed, Type 3: fjords, and Type 4: salt-wedge (Hansen and Rattray Jr. 1966) (Figure 1). In Type 1 the net flow is seaward at all depths and there is a diffusion effect on the upward salt transfer. Type 1a represents a well-mixed estuary where salinity stratification is minimal in contrast to Type 1b where stratification is appreciable. Type 2 is an estuary where the net flow reverses at depth and advection and diffusion contribute to the upstream salt flux. Types 2a and 2b are like Types 1a and 1b, respectively, only for well-mixed estuaries. Type 3 has more influence from advection which can account for over 99% of the

upstream salt flux. Type 3a is the same as Type 3 just with minimal stratification. Type 3b include fjord estuaries where the lower layer is so deep that salinity gradient and the circulation do not extend to the bottom. Type 4 estuaries are salt-wedge, where there is a large degree of stratification and the flow grades from a thick upper layer flowing over a thin lower layer, towards a shallow surface layer flowing with little influence over each gradient (Hansen and Rattray Jr. 1966).

More recently, studies noting inconsistencies in the Hansen and Rattray (1966) stratification-circulation diagram have proposed the addition of nonlinear models and have adapted the diagram, increasing its selectivity to only physically plausible scenarios and to include estuaries with advection-dominated fronts and subtidal salt wedge estuaries (Dijkstra and Schuttelaars 2021). Additionally, the Hansen and Rattray (1966) method did not uniformly distinguish between estuaries with different flow or salinity structures, or dominant salt transport mechanisms therefore, an extended classification diagram using regimes was proposed (Figure 2) (Dijkstra and Schuttelaars 2021). In this classification, models of the four regimes are as follows. Regime 1: dispersive regime, is dominated by a balance between river-induced flushing and dispersive processes for salt import. Regime 2: Chatwin's regime, based on Chatwin (1976) description of a subtidal salt balance between river-induced flushing and import grounded on the interaction between gravitational circulation and the sheared salinity field caused by gravitational circulation. Regime 3: Chatwin's regime with advection dominated front, like Regime 2 but differing in the balance of processes at the salt intrusion limit whereby advection may be the primary mechanism to balance flushing rather than dispersive transport. Lastly, Regime 4: Subtidal salt wedge regime where the surface water is almost entirely fresh, and the bottom salinity decreases on a gradient

close to the mouth before declining rapidly near the salt intrusion limit (Dijkstra and Schuttelaars 2020).

1.1.2. Fjord estuaries

Within a fjord, water masses are generally arranged in three layers; a surface layer, an intermediate layer and a bottom layer (Farmer and Freeland 1983). The surface layer may be well mixed and extends down to the intermediate layers where a steep halocline is present. The bottom layer sits below the depth of the sill and is near freezing. The arrangement of these three layers have been documented in fjords with and without deep-sills (Cottier et al. 2010).

The upper layer is characterized by freshwater, likely from ice melt and runoff. Because of this discharge and surface warming, this layer typically experiences seasonal variability in salinities and temperatures (Cottier et al. 2010). The intermediate layer is often influenced primarily by advected water masses, external to the fjord. It is likely that mixing with shelf waters has occurred and this layer can be relatively warm. The deepest water mass is the densest and often exhibits the highest salinity.

Arctic fjords are subject to seasonal hydrographic cycles. A study of Kongsfjorden in Spitsbergen builds on the previous categorization of a three layer system and provides a general characterization of seasonal fluctuations within arctic fjords (Tverberg et al. 2019). In autumn and winter, the water within the fjord is strongly cooled at the surface through atmospheric heat loss. Convection begins with the formation of sea ice causing surface waters to cool and become increasingly saline from the release of brine (Tverberg et al. 2019). This convection reaches the bottom in the fjord in periods of intense freezing, producing Winter Cooled Water. The presence

of spring causes sea ice to melt forming a low-density surface layer. The depth of this freshwater layer increases with wind-driven mixing and is influenced by surrounding rivers. The low-density surface water increases vertical stability and flows out of the fjord. Below the surface water, Intermediate Water is formed through mixing with the deeper water mass. The steep halocline persists in the Intermediate Water similar to the intermediate layer described by Farmer and Freeland (1983).

Additionally, Tverberg et al. (2019) found that the seasonal cycles within Kongsfjorden may vary depending on which type of winter water production had been dominating. Characterized by three different winter scenarios; Winter Deep, Winter Intermediate and Winter Open winters. Winter Deep winters exhibit convection that extends to the bottom with either little or no advection of Atlantic water into the fjord (Tverberg et al. 2019). The deep convection leads to dense bottom water that causes summer advection of Atlantic water to occur at an intermediate depth. Winter Intermediate winters are defined by winter convection being limited to an intermediate depth and winter advection of Atlantic waters into the deepest part of the water column (Tverberg et al. 2019). Advection of Atlantic water continues to be deep even into summer which results in relatively cold water at an intermediate depth. Winter Open winters are characterized by upwards advection of Atlantic water into the surface layer and winter convection of Atlantic water to the bottom. The summer cycle resembles that of Winter Deep winters except for a shallow Atlantic water advection due to dense winter water (Tverberg et al. 2019).

Understanding the natural variability within fjord estuaries is critical for water resource management, especially in areas manipulated by the development of hydroelectric power

(Montagna et al. 2013). Hydroelectric projects reduce the inflow of freshwater in estuaries while also influencing seasonal variation of inflow pulses (Clarke et al. 2008). Though many of the species found in estuaries are euryhaline and have evolved over long periods of time to be tolerant to changes in freshwater inflow, most remain in locations within their salinity range. Changes in the timing and/or amount of freshwater inflow have thus been observed to affect abundance and distribution of estuarine fish (Carassou et al. 2011; Dadswell et al. 2018; Rytwinski et al. 2020). Fish that enter areas with altered flow regimes may have their sensory-response system impaired from not being able to effectively use their lateral line to sense obstacles and adapt to the complex pressure regimes of hydro turbines (Coutant and Whitney 2000). A quantitative study found that the three main mechanisms that render fish susceptible to dam impacts were 1) transformation of upriver habitats from a lotic or rapidly moving environment to a lentic or still environment; 2) habitat fragmentation and 3) the introduction of non-native species (Turgeon et al. 2019). Additionally, Linear Mixed Effects Models have been applied to investigate the effects of dams on species richness and biodiversity across different biomes (Turgeon et al. 2019). Results have found significant declines in the tropics, lesser affect but similar declines in temperate regions and no changes in boreal regions (Turgeon et al. 2019).

1.1.3. Habitat use in estuaries and biodiversity

Estuaries are some of the most biologically productive and highly diversified areas on Earth (Costanza et al. 1998). Productivity is driven by estuarine circulation which transports nutrients, sediments, and organic materials throughout the entire system. This circulation has a significant impact on energy transfer throughout estuarine food chains, and the abundance and distribution of species that inhabit the area (Murawski et al. 1980; Stoeckle et al. 2017; Kamula et al. 2017; Becker

et al. 2017). These processes facilitate diverse environments with bacteria, phytoplankton, zooplankton, animals, and plants from both freshwater and saltwater ecosystems that increase the diversity of the ecosystem. Additionally, the vertical stratification between water masses promote biodiversity by creating a unique habitat that offers a throughfare for migratory species as well as a nursery habitat for juvenile fish (Blaber and Blaber 1980; Paterson and Whitfield 2000; Bradbury et al. 2008; Simo-Matchim et al. 2016; França and Cabral 2016; Sylvester et al. 2018).

Biodiversity is an important metric for ecosystem monitoring where it is used to quantify and assess the species richness in each area. A diversity index is a quantitative measure that reflects the number of different species and how evenly distributed individuals are among species. There are a few different methods of quantifying the diversity index such as Simpson's Index and the Shannon - Weiner Index.

Simpson's Index (Simpson 1949) was developed in 1949 and is computed as:

$$D = 1 - \frac{\sum n(n-1)}{N(N-1)}$$

Where *n* is the number of individuals of one species and *N* is the total number of all individuals. This index is a weight arithmetic mean of proportional abundance and measures the probability that two randomly selected individuals from the same sample will be the same species. The value of *D* ranges from 0 to 1, where 0 represents infinite diversity and 1 represents low diversity

The Shannon-Weiner index was developed in the late 1940's (Shannon 1948). The index relies on the assumption that the degree of uncertainty of predicting the species of a random sample is related to the diversity of the community. This means that is a community has low diversity, the uncertainty of prediction is low and vice versa.

The most common formula is as follows:

$$H' = -\sum_{i=1}^{s} p_i \ln p_i$$

Where *H'* is the species diversity index, s is the number of species, and p_i is the proportion of individuals of each species belonging to the i^{th} species of the total number of individuals. The higher the *H'*, the higher the species diversity.

Despite both these methods being used widely in ecology, there are some challenges with attempting to quantify diversity within a community. Something these indices lack is the ability to capture abundances of rare species because the diversity values are estimated from biased measures of diversity of the larger community. Two methods that have been put in practice to create more robust diversity estimates are coverage and Hill diversity (Roswell et al. 2021). Coverage is a tool for equalizing samples and is preferred over the commonly used equal-effort sampling. Hill diversity involves a wide range of diversity metrics and is based on three parameters; 1) species richness and variants of the Shannon and Simpson indices are all incorporated into one equations, 2) the richness of Shannon and Simpson indices can be expressed on the same scale with units of species, and 3) "leverage" a concept detailing that the removal of the effect of relative abundance form estimates of any diversity metrics is not permitted so the researcher much choose the relative sensitivity of the metric towards rare species (Roswell et al. 2021).

1.1.4. The Lake Melville Estuary

Lake Melville is a large (2,100 km^2) sub-arctic estuarine fjard (irregularly shaped fjord) that is part of the Hamilton Inlet, on which Innu and Inuit rely for subsistence harvesting (Durkalec et al. 2016). The estuary is the single largest body of water in Labrador, stretching 250 km (Figure 3). The Lake Melville system includes a relatively shallow bay (~55 m) in the western end of the lake called Goose Bay, a small strait with a shallow sill connecting Goose Bay and the eastern upper part of the lake, referred to as the Narrows, and a small Middle portion of the Lake with salinities between 5-10 acting as a transition area from the rest of the system to Upper Lake Melville (~200+ m). Another strait called the Rigolet Narrows separates Lake Melville from Grosewater Bay and the open Atlantic Ocean (Figure 3).

As in other estuaries, river inflows are responsible for regulating physical and ecological processes of the Lake Melville's riverine ecosystems and are characterized by the magnitude of discharge, duration, frequency, timing, and rate of change of flow conditions (Poff et al. 1997). Lake Melville's hydrology is driven by a fjord estuarine circulation (Hansen and Rattray, Type 3b), where brackish surface waters from river run off (salinity <10) flow seaward and the bottom saline waters of the Labrador Sea (salinity ~28) flow landward. These dynamics are primarily driven by two key factors; the vast amount of freshwater input which lowers the surface salinity and energetic tidal mixing at the sill near the Rigolet Narrows (Durkalec et al. 2016). Stratification of the low salinity surface waters (~2 – 20 m deep) and saline bottom waters is very pronounced close to the mouth of the Churchill River and gradually breaks down towards the Labrador Sea (Bobbitt 1982;

Lu et al. 2013). However, the steep halocline persists throughout the year creating a boundary layer between freshwater and saltwater (Durkalec et al. 2016).

Surface currents in Lake Melville approach 0.5 m/s and vary (Durkalec et al. 2016). Past 50 m the currents decrease to around 0.1 m/s, however significant currents (greater than 0.2 m/s at depth and greater than 0.7 m/s at the surface), may be observed at any point of the year. About half (55%) of the variance observed in currents at depth can be attributed to tidal currents (Durkalec et al. 2016). Surface water exchanges within a matter of tens of days, and the residence time of water (time of waters cycling in lake) increases with depth. Complete flushing time has been estimated to be 192 days (Durkalec et al. 2016). Seasonal ice coverage (December – May) increases the strength of tidal currents from the surface to the bottom, whereas in summer the strongest tidal currents are present near the surface (Durkalec et al. 2016).

The generation of power through hydroelectric dams have been extensively criticized for causing disruptions in river flow resulting in the alterations of natural flow characteristics (Clarke et al. 2008). Hydroelectric development involves the generation or flooding of an area to control high and low flows resulting in the absence of high flushing flows which may create high depositions of fine sediments which further affect estuarine biota (Renöfält et al. 2010; Wu et al. 2019). Lake Melville saw changes in the seasonality of freshwater run off after the construction of the Churchill Falls hydroelectric project on the Churchill River in 1971 (Durkalec et al. 2016). Though there was no significant change in the annual mean volume of river discharge, the large pulse of freshwater occurring in late spring/ early summer from ice melt was significantly reduced (~30% decrease) past 1971 (Akenhead and Bobbitt 1986). Moreover, flow rates from December to April

have tripled since before the hydroelectric development (Akenhead and Bobbitt 1986). The new Muskrat Falls hydroelectric project may further influence changes in flow like that of the Churchill development where seasonal flow changes were dampened. However, without evidence from future monitoring we can only hypothesize that two dams will continue and possibly amplify the amount of freshwater delivered into Lake Melville, rather than only having a large influx during the spring ice melt. Increasing year-round freshwater may cause ecological disturbances especially on biodiversity and species who use the seasonality of the estuary for life history cues (i.e. Rainbow smelt).

1.1.5. Fish community in Lake Melville

The first report of Labrador's ichthyology was collected by Horatio R Storer in 1850. Since then, a few species descriptions have been conducted documenting the occurrence of freshwater, marine, and anadromous fish species. Backus (1957) hypothesized that the dispersion of freshwater species into Labrador was achieved by either an eastward dispersal from Hudson Bay or northward and eastward spread from the lower St. Lawrence. Due to the similar freshwater assemblages of the St. Lawrence, dispersal from the St. Lawrence into Labrador is more likely. However, the freshwater fauna of Hudson Bay is rich and the freshwater species of Labrador closely followed the retreating ice sheet, hence an early connection with Hudson Bay may have led to some of the dispersion (Backus 1957).

Historical reports on Lake Melville's species assemblages parallel more recent reports. Common freshwater species are Brook trout (*Salvelinus fontinalis*), Longnose sucker (*Catostomus Catostomus*), and Lake chub (*Couesius plumbus*). Common marine species present in Lake

Melville are Daubed shanny (*Leptoclinus maculatus*), Snake blenny (*Lumpenus lumpretaeformis*), Newfoundland eelpout (*Lycodes lavalaei*), Sculpin spp. (Cottidae), Poachers (Agonidae), American plaice (*Hippoglossoides platessoides*), Winter flounder (*Pseudopleuronectes americanus*) and Tomcod (*Gadus tomcod*). Additionally, anadromous species that frequent the system are Atlantic salmon (*Salmo salar*), Rainbow smelt (*Osmerus mordax*), and Three-spined stickleback (*Gasterosteus aculeatus*) (Backus 1957).

Species that have been reported in Lake Melville but are either rare or data limited include Blue fin tuna (*Thunnus thynnus*) (Backus 1957), Atlantic Cod (*Gadus morhua*), Capelin (*Mallotus villosus*), and Arctic char (*Salvelinus alpinus*) (McCarthy and Gosse 2015, 2018).

Prior to the development of the Muskrat Falls hydroelectric project, while Rainbow smelt were still present, the most abundant species within the tributaries below Muskrat Falls were Three-spine stickleback with White sucker accounted for the majority of the biomass (McCarthy and Gosse 2015). In Goose Bay and Lake Melville the most abundant species was Longnose sucker while brook trout had the highest biomass catch-per-unit-effort (CPUE) (McCarthy and Gosse 2015).

Another abundant species, Rainbow smelt (*Osmerus mordax*), is routinely caught in monitoring efforts in Goose Bay and Lake Melville and as part of the local recreational winter fishery. There, Rainbow smelt has a higher trophic level than other pelagic fish such as Tomcod, but a lower trophic level than predators such as Ringed seals (McCarthy and Gosse 2018). Isotope analysis in the lake confirmed that Rainbow smelt are opportunistic feeders and primarily fed in the estuary

as adults with the bulk of their diet containing decapods and amphipods (McCarthy and Gosse 2018). Because they are the direct link between macrozooplankton and larger fish, marine mammals, and seabirds, Rainbow smelt are considered a forage species that funnels energy throughout the food web. Though smelt are anadromous, moving into freshwater rivers and streams to spawn in the spring, McCarthy and Gosse (2018) have reported no records of adult Rainbow smelt in the Churchill River during late summer and fall sampling; however, recent monitoring has identified infrequent occurrences in the lower portion of the river (McCarthy, unpublished data). As hatched larvae grow, they move into higher salinity waters and gradually distribute themselves to deeper areas within the estuary where they feed from summer to fall (McCarthy and Gosse 2018). Juveniles will then mix in with adult schools and move into upper parts of the estuary in winter (McCarthy and Gosse 2018). Because Rainbow smelt play an integral role in carbon transfer and their life history is highly dependent on the freshwater inflow, monitoring the distribution of the species will not only provide information on the resident population but may also provide inferences on the health of the Lake Melville system.

1.1.6. The role of sentinel species

Attempts at monitoring the state of a particular ecosystem and its respective responses to natural and anthropogenic stressors have been historically difficult to quantify. “Bioindicators” are biological processes, species or communities used to monitor the quality of an environment and how it responds to change. The ecological concept of using a bioindicator species or sentinel species was first used in the early 1900s and has since been applied to various situations including industry compliance with specific laws (Bonanno and Orlando-Bonaca 2017), habitat assessments (Canterbury et al. 2000) and long-term monitoring of the integrity of watersheds (Baos et al. 2022).

Ecologist have set a broad range of criteria that a species must exhibit to be considered a bioindicator. These include good indicator ability, abundant and common, well-studied, and are culturally important (Carignan and Villard 2002).

For a sentinel species to have good indicator ability, they must be sensitive to environmental disturbances and/or stress without experiencing mortality. The response to the stressor may reflect the response elicited by the whole population and be used as a proxy for ecosystem response and be scaled to the degree of degradation of the stressor (Carignan and Villard 2002). Sentinel species are often abundant within the study area and a broad range of animals can act as sentinel species. Invertebrates have been successful sentinel species in heavily trafficked ports such as the Nutclam (*Nucula proxima*) in the Port of Saint John, NB (Pippy et al. 2016) and seabirds such as Common terns (*Sterna hirundo*) have been useful in marine environments (Scopel et al. 2018). Though less popular, fish have also been used as bioindicators for estuaries. For example, in the Iberian Peninsula, a Brazilian silverside (*Atherinella brasiliensis*), a flounder (*Platichthys flesus*) and a mullet (*Mugil cephalus*), are considered estuarine sentinel species. These were selected because their ecology and life history is extensively documented, they are easily studied, and their lifestyle make them particularly vulnerable to the threat being studied (Ferreira et al. 2004; Salgado et al. 2019). Additionally, species that are already harvested for other purposes or are culturally significant and already have public interest and awareness are good candidates for sentinel species to ensure longevity in the monitoring (Carignan and Villard 2002).

Methods for monitoring estuarine ecosystems

1.2.1. Hydroacoustics

The use of acoustics in fisheries science has become increasingly popular as it offers a less-invasive method for monitoring fish populations and increased spatial resolution that is not subject to avoidance such is seen with nets (MacLennan and Simmonds 2013). Historically, the state of fisheries resources was exclusively studied using traditional fishing practices (i.e., trawling, netting) which inadvertently catch non-target species. Integrating acoustics into fisheries monitoring is also highly adaptable to a number of aquatic environments where alterations to the survey design can be optimized pre (e.g., transect design and frequency selection) and post (e.g., noise removal algorithms and multifrequency differencing) processing of acoustic data.

The foundation of hydroacoustics centers around sound theory. Sound travels faster in water (approximately 1480 m/s) than in air (343 m/s) and can reach depths far greater than light. The acoustic equipment or *echosounder* can generate, amplify, and transmit acoustic pulses. When these pulses reach a target the interaction results in a reflected or scattered wave and when part of the scattered wave travels back to the echosounder, it converts the sound energy to voltage and is received as *backscatter* (MacLennan and Simmonds 2013; Demer et al. 2015). There are different types of echosounders each with their own advantages and disadvantages. Single-beam echosounders, as their name suggests, only produce a single beam. They cannot be used to locate targets because the signal is dependent on already knowing the direction of the target and they have to rely on echo statistics to estimate Target Strength (MacLennan and Simmonds 2013). Dual-beam and split-beam echosounders are two instruments that offer a more sophisticated

direct measurement for target strength. Dual-beam echosounders have transducers of 73 elements arranged in four concentric circles around one element at the center (MacLennan and Simmonds 2013). These elements allow for the use of a narrow or wide beam depending on which elements the user has configured to operate. Comparatively, split-beams have a transducer that is divided into three or four quadrants where target direction is determined by comparing the signals received by each quadrant (MacLennan and Simmonds 2013).

Echosounders are used to observe fish in most of the water column besides the near field zone and just above the seabed in the Integrated Dead Zone (IDZ) (Ona and Mitson 1996). The near field is the region immediately below the transducer face and occurs at ranges where the wave-fronts produced by the transducer elements are not parallel (Simmonds 2005; Abraham 2019a). The depth of the near field varies for each echosounder and environment and depends on the wavelength, the wave number (k) and the active radius *a*, this is approximately 5m for a 38kHz transducer. The IDZ region includes the Acoustic Dead Zone (ADZ) and is where fish cannot be detected due to the additive effects of the unsampled volume of a spherical acoustic beam, the acoustic backstep used to exclude signal reflections from the seabed, and the partial integration zone (PIZ) where only a fraction of the echo is detected (Mello and Rose 2009). Hence, limiting the effectiveness of acoustics on studying species that frequent the surface and seabed.

The Sonar equation is used to measure the ratio of sound reflected by a target (i.e. backscatter). This equation incorporates the effect of each part of the remote sensing application on the "power" in the signal of interest (Abraham 2019b). The sonar equation is formulated using the decibel logarithmic scale to accommodate the large dynamic range of acoustic signals and differs

depending on the intended use (i.e., passive, or active sonar equation). Because this study incorporates active sonar, we will be discussing this version of the equation in more detail.

In active acoustics, transducers of echosounders have two main functionalities; converting electrical energy into a transmitted acoustic pulse, or pressure wave, (i.e., a ping), and then the subsequent conversion of pressure waves to electrical signal from the detection of sound reflected off an object. The active sonar equation accounts for the effect of an additional propagation leg from the sound source to the target object and is as follows:

$$SNRa = SL - PLa + TS - PLb - NL + AG$$

Where SL is the source level of the sound projector. PL_a and PL_b is the propagation loss from the sound projector to the target object and from the target object to the sensory array, respectively. TS is the target strength, NL is the total noise power level in the processing band and AG is the array gain in decibels (Abraham 2019b).

As the ping travels outward from the transducer, the wave disperses over a larger area (Figure 4). Because the total energy of the transmission is fixed, the intensity decreases with range (MacLennan and Simmonds 2013). Past the near-field, the intensity varies with range R in agreement with the inverse-square law:

$$I = I_0/R^2$$

Where I_0 is the intensity normalized to unit range.

When a ping encounters a target, some of the incident energy is scattered which generates a secondary wave that propagates in all directions away from the target (Simmonds and MacLennan 2008). Scattering occurs wherever there is a spatial change of the acoustic impedance $Z = pc$, where Z is impedance, p is the density of the medium and c is the velocity of the soundwave transmitted through the medium. The coefficient of the reflection at a boundary is r_b which indicates the proportion of the incident energy in the reflected wave (Simmonds and MacLennan 2008).

$$r_b = (Z_r - Z_W)/(Z_r + Z_W)$$

Where Z_W and Z_r are the acoustic impedances of water and of the reflector, respectively. The greater the change of Z across a boundary, the stronger the scattered wave. The energy reflected towards the source of sound is labeled as "backscatter" (Simmonds and MacLennan 2008). An object with a boundary across which there is a discontinuity in the acoustic impedance is referred to as a target. Targets that are smaller than the wavelength are subject to the same sound pressure when the incident arrives, whereas the incident sound on larger targets may only be scattered by the surface rather than the volume (Simmonds and MacLennan 2008). When target dimensions resemble that of the wavelength, such as fish, scattering is dependent on the geometric structure and the material properties of the target. In fisheries acoustics, backscattering from targets are often caused by fish swimbladders (a gas-filled organ within the fish's body cavity) that create a large density contrast, and thus impedance, between the gas and the fluid medium (Thompson and Love 1996; Stanton et al. 2012).

1.2.2. Spatial analysis

A key issue when estimating abundance and distribution is estimating the precision and variance resulting from different survey designs. Because acoustic data are collected along transects, the unsampled areas in between these transects need to be interpolated using spatial analyses. Using variogram models offers a solution by measuring the mean variability between any two points as a function of the distance vector between these points (Chiles and Delfiner 2012). Kriging, a geostatistical approach used to map resources, has been applied to fisheries population dynamics and uses variograms to construct local unbiased estimates of minimum variance (Simard et al. 2002; Georgakarakos and Kitsiou 2008; Petitgas et al. 2017). Kriging operates under the assumptions of stationarity (model is regulated around its constant mean) and isotropy (population dispersion around its center of gravity is the same along every direction) (Petitgas et al. 2017). Fish density is a stochastic variable whereby the mean statistical distribution is estimated as an average. In fisheries acoustics, the random nature is derived from the movements of fish and from the intrinsic variability of acoustic propagation and scattering (MacLennan and Simmonds 2013). Although fish tend to aggregate in some areas and to avoid others, the density is a result of stochastic processes which depend on location and time of the observations (Petitgas et al. 2017). Therefore, we lean towards the concept of stationarity if all samples show the same statistical distribution (i.e. uniformly distributed) regardless of time and position (Petitgas et al. 2017). Like kriging, "Ordinary kriging" is used to interpolate between known points, but the difference is that Ordinary kriging is used when the mean is unknown. In that case, the sum of the weights are constrained to 100% ensuring that the mean of error is 0, regardless of what the unknown mean ends up being. This is important because it minimizes the variance so that Ordinary kriging can be used to estimate over a large spatial domain (Chiles and Delfiner 2012).

1.2.3. Ground truthing and environmental DNA

Ground truthing refers to the process of determining what is being remotely sensed, for instance with an echosounder (Petitgas et al. 2017). Challenges associated with hydroacoustic sampling include identifying and measuring the targets responsible for the backscatter. Video imagery has been used to verify acoustic signals but this can be difficult especially in estuaries where there are often areas of high turbidity and strong currents where visibility is low (Berger et al. 2020). Therefore, it is important to pair acoustic signals with ground truthing methods such as biological sampling (i.e., trawling or setting nets) to improve the interpretation of acoustic data.

While conventional capture methods, such as trawling, provide a lot of information on species composition and physiology, they are invasive and prone to selectivity biases. Trawling can produce biases attributed to size selectivity and fish avoidance behaviours that fail to offer a complete picture of the communities. Other nets, such as gill nets, are very selective, but this trait can be mitigated with the appropriate application of varying mesh sizes (Hamley 1975). Momentum plays an important role in the catching effectiveness of gill nets where it is a function of both fish swimming speed and mass (McClatchie et al. 2000). It can be difficult to relate gill net catches to acoustic biomass estimates because they measure flux of fish, rather than density (McClatchie et al. 2000). However, gill nets are useful for confirming the presence of species in the area. Moreover, because gill nets can be vertically stratified, they can provide detailed information on the vertical distribution when comparing with the acoustic data.

Less invasive monitoring techniques, such as environmental DNA (eDNA), have become more popular in recent years due to the easy data collection and high efficiency in identifying species

occurrence (Easson et al. 2020). Environmental DNA is a tracer method and is performed by extracting DNA from air, soil, or water samples (Taberlet et al. 2012). This technique does not require sampling individual organisms and can be standardized to estimate false positive and negative detections using molecular practices (Taberlet et al. 2012). Environmental DNA has been reliably applied in freshwater (Mauvisseau et al. 2018), marine (Rooyen et al. 2021), and dynamic river systems and estuaries (Zou et al. 2020; Hallam et al. 2021) and it has also been used in combination with traditional netting/trawl surveys to assess distribution and detection of aquatic species (Berger et al. 2020). Where only small traces of biological tissues or cells need to be present in water samples to be picked up by the analysis, a key advantage to eDNA is that it can detect species that are present in aquatic ecosystems in low abundance. The persistence of eDNA is variable and depends on the environment (i.e. temperature and acidity), but it is said to persist in an aquatic ecosystem for up to 21 days (Dejean et al. 2011). There are additional challenges for applying eDNA in environments with flowing water as tissues can be transported downstream. Understanding the distance from the source population that a species is detectable through eDNA is still not well understood. Along with the aforementioned factors affecting the persistence of tissue, seasonality may also be an obstacle. A study in Lake Greifensee, Switzerland attempted to quantify the eDNA detectability range of two invertebrates within the lake system and found a difference in the seasonal detectability (Deiner and Altermatt 2014). They found that *Daphnia longispina* was present at all sites and seasons but *Unio tumidus* was not found past 9.1 km downstream and 1.6 km in July and then found in October (Deiner and Altermatt 2014). Additionally, the authors estimated the movement of eDNA to be approximately 10 km away from the source, suggesting that the use of eDNA can provide a relatively high resolution (km) in river systems (Deiner and Altermatt 2014).

Rationale and research objectives

The Fish DIP project (Dam Impact on Pelagic Fish) led by the Fisheries and Marine Institute of Memorial University took place between 2018 and 2021. With the goal of providing baseline information on habitat, diversity, distribution, and ecology of pelagic fish inhabiting the Lake Melville system, the Fish DIP project facilitated two complementary master's research projects completed by Jordan Sutton (MSc.) and myself. Sutton's thesis studied the phenology and growth rate of Rainbow smelt to achieve a finer look into the ecology of a high trophic level forage fish. In comparison, the primary objective of my study is to test how seasonal and spatial (i.e., horizontal, and vertical) variations in hydrography influence the abundance, distribution, and diversity of adult and larval fish populations in Lake Melville. We hypothesize that the strong water mass stratification in Lake Melville provides a freshwater refuge for Rainbow smelt larvae (*Osmerus mordax*). Additionally, this study supplements previous biodiversity studies by using eDNA in addition to nets to document the fish community. I thus provide new baseline information on the occurrence and distribution of freshwater, marine, and anadromous species in upper Lake Melville on which to measure future changes.

Chapter 2: Strong water stratification drives the distribution of pelagic fish in a sub-arctic estuary (Lake Melville, Labrador)

Abstract

Estuaries provide nurseries for juvenile fish that rely on the interaction between fresh- and saltwater. The 250 km long Lake Melville spans 2100 km^2 and is the largest estuary of Labrador (northeastern Canada). This sub-arctic fjard hosts freshwater, anadromous, and marine fishes on which depend marine mammals and seabirds, but also coastal communities. The recent completion of a large hydroelectric project on the main affluent of Lake Melville could alter the seasonal flow of freshwater and, ultimately, fish distribution. Yet, the importance of the low salinity surface layer as a habitat for fish remains unknown. By pairing seasonal hydroacoustic surveys conducted in summers 2018-2019 and winters 2019-2020 with net sampling and environmental DNA (eDNA) analyses, we test the hypothesis that the strong water stratification prevailing in upper Lake Melville provides a nursery for early life stages of fish, where they are protected from their predators. Ichthyoplankton aggregated just above and at the pycnocline, in the low salinity surface layer down to 25 m. Most adult pelagic fish occupied the bottom waters below the sharp pycnocline, although some ventured in the low salinity surface layer. Ten species of fish were captured in gill and fyke nets and 53 species were detected with eDNA. Larvae of rainbow smelt (*Osmerus mordax*) were ubiquitous in July and August and represented 100% of the ichthyoplankton assemblage sampled during these months. No fish larvae were detected in winter (February). We conclude that the low salinity surface layer provides a refuge for rainbow smelt larvae, a key forage species in the estuary. This study provides baseline information from which to assess future changes in biodiversity and distribution of fish in the Lake Melville estuary. It

further supports the use of eDNA as a complementary tool for monitoring fish diversity in sub-arctic estuaries.

Introduction

Lake Melville is the largest estuary in Labrador (northeastern Canada). By its relatively shallow and large embayment and its highly stratified water column, it is a typical sub-arctic fjard. Freshwater, anadromous, and marine species cohabit in the Lake Melville estuary and migratory fish species, such as Arctic char (*Salvelinus alpinus*) and Atlantic salmon (*Salmo salar*), use riverine tributaries for spawning and for juvenile nursery habitats (Backus 1957; McCarthy and Gosse 2018). Lake Melville was identified as an Ecologically and Biologically Significant Area (DFO 2013) but, despite its ecological importance, several knowledge gaps subsist on the biodiversity and seasonal variation of fish distribution in in the estuary. Information on fish populations is limited to abundance and distribution from net surveys conducted in summer (McCarthy and Gosse 2018) and, overall, the effects of changes in freshwater inflow on fish productivity remain poorly documented, especially across seasons (Rytwinski et al. 2020)

The Churchill River is the main tributary of Lake Melville and contributes 60% of the freshwater inflow. The seasonality of freshwater inflow was strongly modified by the construction of the Churchill Falls hydroelectric project in 1974, which reduced the natural flow variability and regulated over 75% of the drainage from the total watershed (Durkalec et al. 2016). These changes have resulted in a higher discharge in Lake Melville in winter and a lower discharge in late spring and summer as well as changes in ice formation in winter compared to pre-development (Durkalec et al. 2016). The additional harnessing of the Churchill River for the second phase of the Churchill

River hydroelectric development (i.e., the Muskrat Falls project, first freshwater release in winter 2020) could further modify the seasonal freshwater inflow.

The harnessing of sub-arctic rivers results in higher levels of the neurotoxin methylmercury and, to date, most research on the impacts of the Churchill River hydroelectric development on biota of the estuary has been dedicated to its bioaccumulation (e.g. Anderson 2011; Schartup et al. 2015). However, hydroelectric dams have also been attributed to habitat fragmentation and decline in biodiversity (Wu et al. 2003; Liu et al. 2019b, 2019a). In addition, modifications to the freshwater inflow can alter life history events as well as initiate behavioural and morphological changes in estuarine fish (Clarke et al. 2008). Yet, the exact implications of a modified freshwater inflow on Lake Melville's marine ecosystem remain unknown.

The distribution of fish in the estuarine environment primarily depends on the local hydrography and their ontogeny and swimming ability. The latter varies between species, size, and developmental stages (Tzeng and Wang 1993). Sexually mature fish can modify their distribution by choosing spawning areas and depths that will increase the fitness of their offspring (Iles and Sinclair 1982; Grote et al. 2012; Sundby and Kristiansen 2015). Buoyancy varies with temperature and salinity and strongly affects the vertical distribution and the dispersal of fish eggs (Sundby 1990). Early life stages of most pelagic fish have evolved to adapt their specific gravity and vertical distribution to remain within the pycnocline; a layer where the water density increases rapidly with depth (Sundby 1990; Sundby and Kristiansen 2015). Previous studies have also revealed higher larval species richness and abundance in frontal habitats, such as haline tidal-mixing fronts, with most larvae remaining close to the surface (Sánchez-Velasco et al. 2012). In Newfoundland, the

larval dispersal of estuarine rainbow smelt larvae (*Osmerus mordax*), one of the most abundant pelagic fish in Lake Melville, is closely linked to the hydrography and seasonal changes in estuarine inflow and outflow (Bradbury et al. 2006). There, the positive buoyancy and passive swimming ability of the larvae may explain their surface aggregations above the pycnocline. In some estuaries, turbidity can also be an important driver of the distribution of early life stages of fish because it promotes increasing feeding success (Blaber and Blaber 1980).

In summers 2018 and 2019 and winters 2019 and 2020, we surveyed Lake Melville to assess the biodiversity and seasonal distribution of pelagic fish in relation to its hydrography. Here, we combine environmental and hydroacoustic data, ichthyoplankton and fish net samples, and water sampling for environmental DNA (eDNA) to test the hypothesis that the strong water stratification prevailing in this sub-arctic estuary provides a refuge for early life stages of fish. We further provide baseline information to assess the impacts of future changes in freshwater inflow and water stratification on the pelagic ecosystem of the region.

Methods

2.3.1. Study area

Lake Melville is a 250 km long and 2100 km^2 subarctic estuarine fjard. In contrast to fjords, fjards are defined by irregular bathymetry and low watershed topographic relief (Kamula et al. 2020). The maximum depth of Lake Melville reaches 256 m with a mean depth of 84 m (Figure 5). The Churchill River flows eastward into Lake Melville via Goose Bay and the Goose Bay Narrows (referred to as the Narrows hereafter) that connects to Lake Melville through a shallow (8m) and narrow (2.5km) sill. At its eastern end, Groswater Bay connects Lake Melville to nutrient rich bottom waters from the Labrador Shelf through a narrow (2.8km) sill at the Rigolet Narrows (not

shown on the map). The 30 m deep sill restricts seawater exchange between Groswater Bay and Lake Melville (Durkalec et al. 2016).

Lake Melville's hydrology is characterized by estuarine circulation, where brackish surface waters from river run off (salinity <10) flow seaward and the bottom saline waters of the Labrador Sea (salinity ~28) flow landward. The estuary is seasonally ice-covered (December – May) and semi enclosed with a low-salinity surface layer within the first 10 – 20 m (Bobbitt 1982; Lu et al. 2013). Stratification of the fresher surface waters and saline bottom waters is more pronounced near the mouth of the Churchill River and gradually breaks down towards the Labrador Shelf. The steep halocline persists throughout the year creating a consistent boundary layer between freshwater and saltwater (Durkalec et al. 2016).

2.3.2. Survey design

To optimize the sampling near the mouth of the Churchill River, the survey was concentrated in Goose Bay (GB) and the western part of Lake Melville (termed Upper Lake Melville or ULM, hereafter), from 60° 21.0'W to 59° 36.6'W. In summer, the survey was conducted onboard the R/V *Gecho II* from June 30th to July 12th in 2018 and July 4th to July 14th in 2019. Summer surveys were conducted after the appearance of the swim bladder in juvenile rainbow smelt, occurring within the first 14 days after hatching (Belyanina 1969). The acoustic transects followed a stratified sampling with systematic samples nested within eastern and western strata (Parker-Stetter et al. 2009; Rudstam et al. 2009) (Figure 5). Surveys were conducted during daylight only. Acoustic transects were conducted at vessel speeds of 4-6 knots. Environmental data and net samples were collected at 10 stations distributed from the head of GB towards the western end of ULM. In

winter, the acoustic and environmental surveys were limited to the fixed stations because complete ice cover made continuous transects impossible. The location of winter stations differed slightly from summer stations to avoid dangerous ice conditions (Supplementary Table 1). The study area was divided into two regions (GB and ULM) divided by the shallowest point (~ 1.5 m) of the Narrows (60° 2.4'W, 53° 27.0'N to 59° 58.2'W, 53° 24.0'N). Permission to conduct this research was granted by the Nunatsiavut Government, Innu Nation, and the NunatuKavut Community Council prior to the first sampling operations.

2.3.3. Environmental data

Conductivity, temperature, and depth (CTD) profiles were collected at each station using a calibrated CastAway-CTD (summer), a vertical microstructure profiler (Model VMP-250) from Rockland Scientific International (winter 2019 and 2020) or an RBR Concerto^3 (winter 2019 and 2020, respectively). Turbidity and Chlorophyll-*a* (chl-*a*) data were also collected for all winter 2019 stations using the VMP's JFE Advantech Co. Fluorescence and Turbidity (JFE-FT) sensor. The manufacturer's calibration were used for this sensor and measurements are expressed in formazine turbidity units (FTU) for turbidity and part per billion (ppb) for chl-a (uranine reference).

Temperature, salinity, turbidity, and chl-*a* data were cleaned to omit the first meter of samples and to only include valid down casts. The conservative temperature (θ), the absolute salinity (S_A) and the density anomaly referenced to the surface (σ_0) were derived using the TEOS-10 toolbox (McDougall and Barker 2011). The data were then vertically binned (averaged every 25 cm). The depth of the pycnocline was estimated for each station by calculating the maximum difference in

water density between two depths and averaged by region (i.e., ULM and GB). These depths were then used to distinguish the average temperature and salinities for the surface ands bottom layers (i.e. above/below the pycnocline) for the two regions and for all sampling seasons.

Year-round environmental data were collected by a permanent mooring (53° 22.2'N; 60° 07.4'W; depth ~ 37 m) equipped with six HOBO TidbiT® v2 temperature loggers spread over the water column, in addition to a RBR Concerto^3 CTD and a Sea Bird Scientific ECO-FL Fluorometer targeting the near surface layer. During the second year of the deployment, a Seabird CTD replaced the RBR CTD near the surface, and latter was put near the bottom. The mooring was originally installed on July 2, 2019 and serviced 13-14 October 2020 (the ECO-FL fluorometer stopped working on September 26, 2020). During the re-deployment of the mooring, a piece of rope near the bottom-end of the mooring got tangled up with the acoustic release system bringing all instruments down by 3 m from their targeted depths. The second deployment acquired meaningful measurements until 4 October 2021.

2.3.4. Acoustics

2.3.4.1. Sampling and processing

Summer acoustic data were collected continuously (~8 h per day) using a multi-frequency echosounder (Simrad EK60; 38 kHz and 120 kHz) hull mounted on the port side 1 m below R/V *Gecho II*. The ping rate was set to 1 Hz and pulse durations and 3 dB beam angles for each acoustic transducer are detailed in Supplementary Table 2.

In winter, stationary acoustic data were collected from drilled holes across the sea-ice. In winter

2019, acoustic data was collected using a Wideband Autonomous Transceiver (WBAT, 38 kHz) was used and in winter 2020, a portable wideband echosounder system was used (Simrad EK80; 38 kHz Supplementary Table 2). In both years, transducers were fixed 1m below the surface of the ice and recorded data for 45 minutes at each station. All echosounders were calibrated before or after each field season using the standard sphere method (Demer et al. 2015).

Acoustic data were processed with Echoview (version 11.1; Echoview Software Pty Ltd.). The top 5m below the surface were excluded to eliminate the near-field transducer effects (Ryan et al. 2015) and to reduce the noise created from bubbles in summer. The sounder-detected bottom was corrected where necessary and a bottom exclusion line was created to eliminate data within 0.5m from the bottom. The S_v (volume backscattering strength, dB re 1 m^{-1}) acoustic echograms were visually inspected and cleaned using Echoview's algorithms to remove background noise with a signal to noise ratio <10 dB, impulse noise, and attenuated noise signals (De Robertis and Higginbottom 2007; Ryan et al. 2015). Clean acoustic data were integrated into bins 0.50 nmi long and 1 m deep. As a proxy for abundance of pelagic organisms in both summer and winter, the Nautical Area Scattering Coefficient (NASC, s_A in m^2 nmi^{-2}) was integrated at 38 kHz and 120 kHz (summer only) and exported for post-processing.

To map the spatial distribution of pelagic fish in summer and identify potential hotspots, we kriged the integrated NASC values using the "krig" function from the R package GSTAT (Pebesma 2004). To achieve normality, the NASC was converted into Nautical area scattering strength (S_A in dB re $1m^2$ nmi^{-2}). Variograms were chosen based on the best fit model (Spherical, Gaussian, Maternal, or Exponential) using the "fit. Variogram" function from the R GSTAT package (version

1.3.1056) (Pebesma, 2004). To investigate differences in vertical distribution, we also integrated and then kriged the S_A values above and below the pycnocline.

T-tests were used to check for significant differences between the mean S_A above and below the pycnocline and between regions (ULM and GB). Statistical tests were performed using R (version 1.3.1056).

2.3.4.2. Target Strength analyses

Target Strength (TS in dB re $1m^2$) of single targets at 38 kHz were extracted using Echoview's single-echo detection algorithm for split beam echosounders (method 2) with a threshold of -110 dB to include larval fish (Supplementary Table 3A,B). Echoview's fish tracking algorithm was then applied to the single target echograms to extract single fish tracks (Supplementary Table 4). Maximum number of pings between fish tracks were modified to 1 to account for large densities of schooling fish seen on the echograms. We exported the mean compensated TS and the mean depth for each single target track. Percentage of total TS of surface to 25 m and below 25 m were calculated for pooled summers (2018 – 2019) and pooled winters (2019 – 2020). Note that winter TS data come from narrowband in 2019 and from the nominal frequency from wideband signals in 2020, but that there was no significant difference when comparing both years (F = 1.0636, p-value = 0.0572).

2.3.5. Fish sampling

In summer, a consistent sound scattering layer (SSL) was present between ~10 and 25 m on the echograms. At each of the stations, a BONGO net (2 x 28 cm diameters with 335 µm mesh) was

towed at 2 knots in the SSL for 10 minutes. Samples were filtered through a 120 µm sieve. Juvenile fish species were separated from zooplankton and were fixed in 90% ethanol that was replaced after the first 24 hours.

Fish monitoring was completed using double bag fyke nets and experimental gillnets deployed in August 2018 and August – September 2019. All nets were set for 16 hours to include both dusk and dawn periods when fish are active. Fyke nets sat on the bottom, ranged from 0.5-1.5 m in height, and were designed to capture small fish (between 40-50 mm in length) in coastal waters no more than 2 m deep. Experimental gillnets were designed to catch larger fish and consisted of four 50 ft panels (200 ft in total) with mesh size, 2", 3", 4" and 5". Gillnets were deployed in shallow waters no deeper than 5 m. Abundance and biomass in Catch Per Unit Effort (CPUE) were calculated by dividing the number and weight of each individual species by the net soaking duration (16 hr). Shannon-Weiner index as calculated for each region (ULM and GB) and year (2018-2019) except for GB in 2018 when no nets were deployed.

2.3.6. Environmental DNA

2.3.6.1. eDNA collection

Water samples were collected for eDNA analyses during summer 2018. The depth of each sample varied depending on where the most backscatter was observed on the echosounder. For each sample, two litres of water were filtered with cellulose nitrate filter membranes with a 0.45-µm pore diameter. Negative field controls (blanks) using distilled water were completed for every station. These controls were performed in the same field conditions as the samples and processed in the same way to estimate potential contamination. After filtering, the filters were kept frozen and processed in laboratory at Université Laval. Unfortunately, no eDNA analyses were conducted

in winter nor summer 2019.

2.3.6.2. eDNA extraction

DNA was extracted using a QIAshredder and DNeasy Blood and Tissue kit (Qiagen) following a modified manufactured protocol (Goldberg et al. 2011; Spens et al. 2017) Extraction was performed under a UV hood with all instruments either bleached and/or UV-treated. In all extraction batch, an extraction control was included to account for possible contamination.

2.3.6.3. Polymerase chain reaction (PCR) amplification and sequencing

eDNA amplification was conducted using MiFish primers (Miya et al. 2015; MiFish-U-F 5′- GTC GGT AAA ACT CGT GCC AGC-3′ and MiFish-U-R 5′-CAT AGT GGG GTA TCT AAT CCC AGT TTG-3′). These universal primers target a hypervariable region of the 12S rRNA gene (174 bp) designed specifically to amplify and disentangled at the species level all fishes. A single PCR reaction was conducted using dual index Illumina barcodes to reduce contamination. Each PCR reaction was composed of 12.5 µl of MasterMix (Qisgen), 2 µl of each primer (10 µM), 5.5 µl of diH_20, and 3 µl of DNA sample. PCR was run under the following conditions: 15 min at 95^{O}C, 35 cycles (30 s at 94^{O}C, 90 s at 65^{O}C, 60 s at 72^{O}C) followed by a final extension of 10 min at 72 ^{O}C. For each sample, including extraction control, PCR was done in five replicates that were pooled after amplification. In addition, a PCR negative control was included for each barcode combination. PCR products for each sample were pooled and verified on an 1% agarose gel. No amplification was observed in PCR negative controls. Pooled PCR products were then cleaned with AxyPrep Mag PCR Clean-Up kit (Corning) and quantified by fluorescence (Accuclear Ultra High Sensitivity dsDNA Quantification Kit (Biotium)). Samples were then pooled in equimolar proportion, cleaned and fragment size distribution checked on an Agilent 2100 Bioanalyser (High

Sensitivity DNA kit). Sequencing was performed on an Illumina Miseq (Illumina, Nextera XT V3) at the genomic platform of the Institut de Biologie Intégrative et des Système (IBIS) at Laval University (http://www.ibis.ulaval.ca/).

2.3.6.4. Sequence cleaning and annotation

Raw sequencing reads were demultiplexed by the Miseq Control Software. Reads were filtered, merged, and annotated by the Barque pipeline (v1.5.4) developers by Eric Normandeau in Louis Bernatchez' Lab (www.github.com/enormandeau/barque). Species identification was performed using the Mitofish 12S database (Iwasaki et al. 2013), available from the latest BARQUE versions. A minimum of 97% similarity between the sequences of interest and the database sequences was required to assign taxonomic identification.

Non-fish sequences and out of range species (defined as species not documented in Eastern North America) were removed from the analysis. Individual species or sequences attributed to more than one species with numbers of sequences less than 50 were also removed from the analysis. Stations were divided into regions (ULM and GB) and in layers above and below the pycnocline.

Results

2.4.1. Environmental parameters

The Goose Bay / Upper Lake Melville ecosystem is characterized by two water density layers separated by a strong haline stratification across all seasons (Figure 6). The depth of this interface between the two layers, the pycnocline, vary between seasons and regions (Table 1). In Goose Bay, the pycnocline was deeper in the summer (10.4 and 12.9 m for both years) compared to the winter (6 and 7 m). In Upper Lake Melville, the depth of the pycnocline underwent larger

variations, averaging at 7 and 12 m in the summer and 11 and 10 m in the winter for both years, respectively.

The Upper Lake Melville was consistently colder and more saline than Goose Bay for both layers (Table 1). Above the pycnocline a low salinity surface layer (LSSL) was present all year long, with summer salinities as low as 0.8 g kg^{-1} and 2.4-2.7 g kg^{-1} in Goose Bay and Upper Lake Melville, respectively. During the winter, the salinity in the LSSL decreased from 2.1 g kg^{-1} to 0.5 g kg^{-1} between winter 2019 and 2020 in Goose Bay, and from 10 g kg^{-1} to 4 g kg^{-1} in Upper Lake Melville, although the latter has large variations (Table 1). In the bottom layer, salinity was much higher, ranging from 16 g kg^{-1} to 24.4 g kg^{-1} across both regions and seasons. In the context of a water release from the Muskrat Falls dam in winter 2020, it is worth noting that the bottom salinity decreased in Goose Bay and increased in Upper Lake Melville between winters 2019 and 2020.

In the summer, the LSSL was consistently warmer (up to 12.9°C in Goose Bay and 13.1°C in Upper Lake Melville on average) than the bottom layer. The latter was relatively stable in temperature throughout the seasons (between 1.6 and 2.2°C in Goose Bay and 0.5 and 1.1°C in Upper Lake Melville). In winter, the temperature of the LSSL was near the freezing point everywhere. The sill separating Goose Bay from the Upper Lake Melville generally limit the exchanges in the bottom layer between both regions as suggested by the contrasted properties of the bottom layer described above (see also Figure 6).

Turbidity and chl-*a* concentration measurements were available for the top ~20m of the water column in winter 2019 (Figure 7). The turbidity was higher in the LSSL and lower in the bottom

waters. It was also higher in Goose Bay than in Upper Lake Melville, which supports existing literature that have suggested a high turbidity region near the mouth of the Churchill River (Durkalec et al. 2016). Similarly, the concentration of chl-*a* in the surface layer were higher in Goose Bay than in Upper Lake Melville.

The vertical distribution of temperature throughout the water column, as well as the salinity and chl-*a* fluorescence at discrete depths were also measured nearly continuously with a mooring near the mouth of the Churchill River between July 2019 and October 2021 (Figure 8). A warmer surface layer (<15 m) developed annually between June and November, with weekly averaged temperature peaking at about 17°C, before decreasing to freezing point in winter (Figure 8A). In the bottom layer, water temperature remained relatively constant below 4°C throughout the year. Note that the temperature in the bottom layer was colder (<2°C; darker shades of purple) during the winter 2020 compared to the winter 2021. This can be explained by the fact that 2021 was a relatively mild winter in the region (Cyr et al., 2022).

The salinity in the surface layer (measured at 8 m and 11m during both deployments, respectively) remained between 10-17 g kg^{-1} (2019-2020) and 17-19 g kg^{-1} (2020-2021) from the late summer to the following spring where it rapidly dropped near 0 g kg^{-1} at the onset of the spring freshet and the melting season in late May (Figure 8B). The greater values and weaker variability of the salinity during the second year is partially explained by the deeper location of the CTD during the 2020-2021 deployment.

Chlorophyll-a concentrations show clear spring blooms occurring in late May in both years (Figure

8C). These blooms correspond to the rapid freshening of the surface layer discussed above (Figure 8B) and likely associated with sea ice melt and further stratification of the water column. Later in the year, Chlorophyll-a concentrations slowly decrease from the summer values until the next spring, although small increase in the fall (i.e. fall blooms in August-September) are visible. Again, differences in concentration between the two years may be partially explained by differences in the depth of the sensors.

2.4.2. Vertical and spatial distribution of pelagic fish

In summer, a strong sound scattering layer was consistently observed just above and within a depth range close to the pycnocline down to 25 m (Figure 9A). Although the pycnocline was present year-round, the absence of the sound scattering layer in winter (Figure 9B) supports the assumption that it was mainly of biological origin rather than physical (Figure 9). Moreover, while the pycnocline was consistently present across the study area, the distribution of backscatter was patchy, as expected for biological targets. Net sampling within the sound scattering layer confirmed the occurrence of Rainbow smelt larvae at all stations in summer, which composed 100% of the ichthyoplankton community. Between 13 and 241 Rainbow smelt larvae were caught at each station, for a total of 770 and 1129 larvae in summer 2018 and 2019, respectively. During both summer and winter, the echosounder also detected larger fish as scattered targets in the bottom water layer (Figures 9A, B and 10).

In summer, single targets detected at 38 kHz in the top 25 m had a dominant Target Strength (TS) mode at -71 dB re 1 m^2 and a second mode at -52 dB (Figure 10A). Target Strengths below the pycnocline in summer were also bimodal with the highest rate of occurrence centered at -55 dB re 1 m^2 and a second, lower, mode at -71 dB re 1 m^2. In winter, fewer targets were detected in the top

25 m where the mode was centered at -56 dB (Figure 10B). Additionally, in winter most targets were distributed below 25 m and had a TS distribution centered around -56 dB. During both summer and winter, weaker targets were distributed in the top 25 m and stronger targets were concentrated in the bottom layer, at depths >25 m.

Investigating target strength per region showed a mode of -69 dB re 1 m^2 in ULM while in GB there was a bimodal distribution with peaks at -50 dB re 1 m^2 and -66 dB re 1 m^2 in the first 25 m indicating that smaller targets, such as larval fish, are more abundant in ULM than GB (Figure 11A, B). Below 25 m, both regions had a mode of -55 dB re 1 m^2.

In summer, the average backscatter within the LSSL was distributed across the study area and was similar in Goose Bay and upper Lake Melville in 2018 (t-test, t = -0.59031, df = 2812.6, p-value = 0.555; Figure 7A). However, in 2019 Goose Bay had a higher backscatter in the LSSL than upper Lake Melville (t-test, t= 13.56, df = 995.57, p-value <0.05). In the bottom layer, the backscatter was higher in upper Lake Melville than Goose Bay (2018 t-test, t = -54.262, df = 4898.9, p-value < 0.05, 2019 t-test, t = -63.299, df = 5133.5, p-value <0.05) and was concentrated near the main affluents of upper Lake Melville (i.e. Kenamu and Northwest rivers; Figure 7A). The trends were similar at 38 and 120 kHz (Figure 7B). In winter, the backscatter was relatively uniform between LSSL and the bottom layer (2018;t-test, t = 0.44471, df = 9.8218, p-value=0.6, 2019; t = 1.7013, df = 9.4426, p-value = 0.1) with no differences in backscatter within Goose Bay and upper Lake Melville (Figure 12).

2.4.3. Biodiversity of pelagic fish

A total of 275 adult fish were sampled in the gill and fyke nets between August 11-15, 2018, and 211 were caught between August 19- September 27, 2019 (Table 2). Nine species co-occurred: *Salvelinus fontinalis* (Brook trout), *Catostomus Catostomus* (Longnose sucker), *Osmerus mordax* (Rainbow smelt), *Microgadus* tomcod (Tomcod), *Catostomus commersoni* (White sucker), *Couesius plumbeus* (Lake chub), *Gasterosteus acusleatus* (Threespine stickleback), *Pseudopleuronectes americanus* (Winter flounder), and *Cottidae* (mottled, spiny sculpin). All species were sampled both years except for Winter flounder which were present exclusively in 2018 and sculpin which were present in 2019 only. The most abundant adult fish in the nets in 2018 were White sucker and Longnose sucker in ULM (n= 77 and 59, respectively). In 2019 Longnose sucker was the most abundant in ULM (n= 68) (Table 2). Lake chub, Rainbow smelt, Three-spine stickleback, and Tomcod were the only species that were found in both GB and ULM in 2019. Fish diversity measured from net samples was higher in ULM than in GB (Table 3). Note that fyke and gill nets were not deployed in GB in 2018.

2.4.5. Environmental DNA

A total of 8.38 of the 9.40 million sequences obtained from the Illumina Miseq platform were annotated to a species by the Barque pipeline. A total of 53 unique species were identified by eDNA. A total of 53 unique fish species were identified by eDNA, and all species collected in the nets were also detected by eDNA. Fifty-one species were found in the LSSL (above the pycnocline), and 44 in bottom waters below the pycnocline. Overall, 31 marine species, 13 freshwater species, and 9 anadromous species were detected (Table 4). Below the pycnocline, ULM had 42 different species and GB had 22. Overall, 28 marine, 13 freshwater and 9 anadromous

species were found in ULM. There were 21 marine, 12 freshwater and 8 anadromous species detected in GB. Freshwater species made up the top 10% of sequences of each species found in ULM above the pycnocline, while below the pycnocline, the highest number of sequences came from genus Gadus with the second most being freshwater species. In GB, the greatest number of sequences above and below the pycnocline came from the genus Gadus, followed by Pleuronectidae and freshwater species.

Discussion

4.1 The low salinity surface layer and pycnocline of Lake Melville as a habitat for rainbow smelt larvae

In July and August, rainbow smelt larvae formed a ubiquitous sound scattering layer aggregated above and in a depth, range related to the sharp pycnocline separating the low salinity surface layer (LSSL) from the colder and saltier bottom waters. This sound scattering layer was absent in winter, despite the stratification prevailing year-round in Goose Bay and upper Lake Melville. Very few small targets, such as fish larvae, were detected in the bottom layer (Figure 9 C,D), and we deduced that most rainbow smelt larvae remained above and within the pycnocline. The TS mode at -71 dB prevailing in the LSSL and pycnocline in summer would correspond to a 7.4 mm rainbow smelt, based on an equation developed for rainbow smelt at 70 and 120 kHz from Rudstram et al. (2003) (derived from Love, 1977). This is within the size range of the rainbow smelt we sampled (4.9-13.1 mm with an average of 7.7 mm; Sutton 2022) and supports the assumption that the sound scatter layer originates from larval rainbow smelt. The TS analysis suggests that most larger fish remained in the bottom layer (Figure 9). This is supported by eDNA observations from which 57% of the species detected were purely marine and likely prefer to remain in the bottom waters while in the estuary. Based on these results and those from a company paper (Sutton 2022), we conclude

that, in Lake Melville, rainbow smelt larvae hatch in late June - early July at river mouths and move downstream into the estuary where they remain in the low salinity surface layer (this study) until they become juveniles at around 90 days post hatch (Sutton 2022). This behaviour is similar to that from other rainbow smelt populations, for instance on the south east coast of Newfoundland (Bradbury et al. 2006).

While the pycnocline can represent a physical barrier preventing zooplankton and ichthyoplankton from crossing water mass boundaries (Röpke et al. 1993), several ecological advantages could also explain the aggregation of rainbow smelt a the pycnocline. First, the size segregation suggests that predator avoidance partly drives the distribution of smaller fish in the top layers. Similar distribution and behavior has been observed near river mouths where negative geotaxis by rainbow smelt larvae was linked to predator avoidance in natal river systems (Bradbury et al. 2004). Yet, the occurrence of some targets with a TS mode of -52 dB in the LSSL in summer (Figure 9A) suggests that some of the larger fish ventured in the top layer, presumably to feed on larval fish and zooplankton. This would also explain the occurrence of adult fish in the shallow coastal waters, as seen from the fyke and gill net samples. The low backscatter in the LSSL in winter suggests that these upward migrations by adult fish are limited to summertime, furthermore, supporting the idea of a predation behaviour.

Secondly, an abundance of palatable zooplankton at the pycnocline could increase prey encounters for first feeding larvae and cause the larvae to aggregate at the surface. After hatching in fresh or brackish areas, rainbow smelt larvae are passively transported towards the surface and start feeding on Mysis, Daphnids and copepod nauplii just after the resorption of their yolk sack at 7 days old

(Sirois et al. 1998; Stritzel Thomson et al. 2011). These zooplankton were abundant in the LSSL and pycnocline in summers 2018 and 2019 (M. Geoffroy, unpublished data). Zooplankton generally aggregate at the pycnocline because of the consistent density differences of the water masses (Meerhoff et al. 2013; Geoffroy et al. 2017; Pérez-Santos et al. 2018). Additionally, zooplankton are generally abundant in estuarine turbidity maximum (ETM) (Blaber and Blaber 1980; Fuji et al. 2010) and our result demonstrate higher turbidity above the pycnocline. By foraging at the pycnocline rainbow smelt larvae thus increase their feeding success and, ultimately, larval survival and recruitment (Leggett and Deblois 1994; Pepin et al. 2015). These observations emphasize the importance of the freshwater surface layer on the distribution of rainbow smelt larvae. If the changes in seasonal freshwater inflow observed after the lower Churchill hydroelectric project are exacerbated by the operation of the second phase, it may impact the distribution and survival of the zooplankton prey. In turn, it could potentially result in a mismatch between first feeding larvae and the occurrence and distribution of their main prey (Cushing 1990).

In addition to predator-prey interactions, the freshwater refuge hypothesis could partly explain the aggregation of rainbow smelt above and within the pycnocline. Developed for Arctic cod, this hypothesis stipulates that for small pelagic fish hatching in cold waters, such as rainbow smelt in Lake Melville, areas with high freshwater discharge provide a warm thermal refuge for survival of early life stages (Bouchard and Fortier 2011). A similar situation could be at play in Lake Melville where the larvae would have better growth and survival rates in the warmer waters prevailing near the surface from June to October relative to the colder bottom waters below the pycnocline (Figure 6). These larvae would reach a larger size at the onset of the winter, when ice

starts forming, which would result in higher recruitment and selectivity for these individuals (Bouchard and Fortier 2008).

4.2 Fish diversity and distribution

Although we cannot determine relative abundance based on the number of DNA sequences, by combining the eDNA results and net catches we can make inferences on presence-absence and diversity (Lodge et al. 2012; Thomsen et al. 2012; Evans et al. 2017). As expected, the highest number of sequences for freshwater fish, such as longnose sucker (*Catostomus catostomus*), white sucker (*Catostomus commersoni*), and longnose dace (*Rhinichthys cataractae*), were found above the pycnocline and the highest number of sequences for marine species, such as American plaice (*Hippoglossoides platessoides*), Atlantic cod (*Gadus morhua*), and Greenland cod (*Gadus ogac*) were detected below the pycnocline (Table 4). Yet, the DNA of both freshwater and marine species were detected throughout the whole water column, likely due to mixing and drifting of biological tissues via currents (Deiner and Altermatt 2014). Our eDNA results confirmed the presence of 48 species that have previously been documented within Lake Melville and surrounding tributaries (Backus 1957; McCarthy and Gosse 2018; Wells et al. n.d.). Of these 48 species, 11 have rarely been observed in the estuary. These species are American sand eel, burbot, herring, fish doctor, snakeblenny, rock gunnel, Atlantic halibut, Allegheny pearl dace, Atlantic redfish spp., fourline snakeblenny, and Pacific sandlance. Common dab were regularly detected in our eDNA samples, but existing literature reports that the species' northern limit was assumed to be in the Strait of Belle Isle (Backus 1957). Other species detected with eDNA that were reported for the first time in Lake Melville comprise blackspotted stickleback, haddock, prickly sculpin, and mountain whitefish. Although the use of eDNA is not without constraints, our results support previous

studies which concluded that eDNA is a useful complementary tool for monitoring fish diversity and species richness in northern estuaries (Berger et al. 2020; Lacoursière-Roussel et al. 2018).

The net and eDNA data indicate that upper Lake Melville was more biologically diverse, including freshwater, anadromous and marine species, than Goose Bay. The acoustic survey also detected higher backscatter in the bottom layer of upper Lake Melville than Goose Bay in summer. The larger inflow of Atlantic water from the Labrador Sea in upper Lake Melville than in Goose Bay (Durkalec et al. 2016) likely explains higher abundances of marine fish species. The Atlantic water inflow could also result in higher abundance of lipid rich copepods, which in turn would attract fish (Head et al. 2003; Pepin 2013). This hypothesis is supported by the higher acoustic backscatter at 120 kHz, a frequency at which meso- and macrozooplankton dominate the acoustic signal, in upper Lake Melville than in Goose Bay. As for the freshwater and anadromous species present in upper Lake Melville, they may be related to the freshwater inputs from the Northwest and Kenamu rivers. For example, both rivers are known by residents as prime fishing grounds for salmonids (Doug Blake, Northwest River, personal communication).

The higher abundance of pelagic organisms in Goose Bay than upper Lake Melville in winter (Figure 10) is more puzzling. A recreational ice fishery for rainbow smelt occur in Goose Bay during winter and spring and it is possible that rainbow smelt spawn at the mouths of the Churchill and Goose rivers. In winter, the salinity of Goose Bay is lower and the freezing point is higher resulting in higher temperatures (Table 1). Coupled with higher turbidity and primary production (Figure 7), higher winter temperatures in Goose Bay could provide a better habitat for zooplankton and fish (North and Houde 2003). Future changes in seasonal river discharge could alter this habitat

and have consequences on fish distribution and abundance (Blaber and Blaber 1980; North and Houde 2003; Carassou et al. 2011; Peterson et al. 2013). Further studies should also investigate the importance of Goose Bay as a winter habitat for estuarine fish.

4.3 Assessing the impact of further river harnessing

This study complements other baseline studies of Lake Melville (Lu et al., 2013; McCarthy et al., 2015, 2018; Durkalec et al., 2016). Unlike the preceedings, it coincided with the completion of the second phase of the Churchill River hydroelectric development (i.e., Muskrat Falls) and the first winter freshwater release in 2020. In this context, the observed 4-fold decrease in Goose Bay surface salinity between winters 2019 and 2020 is worth noting (Table 1). For the same period, a little more than a two-fold salinity decrease was also observed in Upper Lake Melville surface waters, although with large variations. In the bottom layer, an increase in salinity was observed in Upper Lake Melville in the winter 2020 compared to 2019, which is coherent with increased estuarine circulation and inland pumping of oceanic waters at depth associated with increased river discharge (Saucier et al., 2009). The other physical parameters presented in Table 1 (the depth of the pycnocline and the temperature of both the surface and bottom layers) did not change significantly between the two years of this study. While it can be hazardous to draw any conclusion from such a short time period, these observations emphasize the importance of closely monitoring hyrographic changes in the ecosystem, especially in the context of planned alteration of the natural debit of the Churchill River. In the light of the findings made here, it was decided to leave the mooring at the mouth of the Churchill River to start such monitoring, which hopefully can bring answers to some questions raised in this study.

4.4 Conclusions

This study demonstrates that 1) rainbow smelt is one of the most abundant forage fish in Lake Melville; 2) the distribution of rainbow smelt larvae is closely tied to the physical oceanographic conditions; and 3) eDNA can be used as a complementary tool to monitor fish diversity in sub-arctic estuaries. Rainbow smelt were consistently sampled in the ichthyoplankton nets, gill and fyke nets, and detected in the eDNA samples. The species is known to funnel energy between zooplankton and top predators such as trout, ringed seals, and seabirds (McCarthy and Gosse 2015, 2018). It is also an important cultural species for local communities and a yearly recreational ice fishery targets rainbow smelt. The recent completion of the Muskrat Falls hydroelectric project on the lower Churchill River, the main tributary of Lake Melville, could modify the seasonal inflow of freshwater. This process could already be underway, with an observed decrease in salinity in the winter of 2020 compared to 2019. Our results suggest that, as a counterpart, if the freshwater inflow is reduced in summer it could impact the distribution and, potentially, survival of rainbow smelt larvae. Given the importance of the species for higher trophic levels, any change in the abundance and ecology of rainbow smelt will have cascading impacts on the whole ecosystem of Lake Melville. We thus suggest monitoring the abundance, distribution, and condition of rainbow smelt as a sentinel species for the ecosystem of Lake Melville. Monitoring fish biodiversity, for instance using eDNA, would also indicate potential changes in the ecosystem of the estuary.

Chapter 3: General Conclusions

Because Rainbow smelt are among the most abundant forage fish within Lake Melville, it makes them a relatively easy species to monitor. In our study adult rainbow smelt were found all throughout Lake Melville and Goose Bay. Even though, Rainbow smelt are anadromous, there are no historic reports of Rainbow smelt in the Churchill River and only some observations (~10 individuals) of smelt caught in the lower reaches of Lake Melville and Goose Bay (McCarthy, pers comm). These occurrences could indicate a limit to their habitat range and emphasize their reliance on the stratification present in Lake Melville (McCarthy and Gosse 2018). This is also confirmed by the greater number of specimens caught in Upper Lake Melville (ULM) compared to in Goose Bay. Higher Rainbow smelt abundance in ULM may be attributed to the higher species diversity as shown in this study.

We observed a year-round vertical stratification and clearly demonstrated that the distribution of Rainbow smelt larvae in summer was tied to this stratification. Although it is common to observe plankton in coastal surface waters, we have verified that the acoustic backscatter observed above the pycnocline was likely a mix of plankton, larval fish, and some adult fish. The larval fish was confirmed to be 100% Rainbow smelt while the adult fish were likely to be freshwater tolerant piscivores feeding on the plankton rich layer. We have also confirmed that the signal was biological rather than physical (water mass differences) based on the absence of the SSL in winter.

In addition to nets, environmental DNA (eDNA) was used to ground truth the acoustic signal and provided information on the biodiversity of the fish present within Lake Melville. eDNA has been used to monitor the biodiversity of fish in other estuaries such as the Saguenay fjord, Canada

(Berger et al. 2020), and areas within the Canadian arctic such as Churchill and Iqaluit (Lacoursière-Roussel et al. 2018). The eDNA analyses detected a total of 56 species, 37 marine fish species, 12 freshwater species, and 7 anadromous species were detected with the eDNA. Although we were unable to determine relative abundance with certainty, we can make inferences on species richness with presence-absence confirmed by net catches (Lodge et al. 2012; Thomsen et al. 2012; Evans et al. 2017). The abundance of freshwater species detected by eDNA also emphasizes the degree of freshwater influence to Lake Melville and Goose Bay which can be a useful tool for future monitoring as the area is subject to anthropogenic changes.

The next steps should be to incorporate standardized practices for ground truthing methods such as setting net catches in all four seasons, not just summer. It is likely that more seasonal data would provide a higher degree of data resolution for estimating species diversity and distribution, specifically for anadromous fish populations that use Lake Melville as a throughfare. It is recommended that turbidity measurements and chlorophyll-a concentrations be consistently taken for water quality monitoring and to better infer the degree of primary productivity within the system. Additional focus on collecting eDNA should also be applied as a non-invasive method for determining the presence of species. Future studies should also expand the study area to encompass the lower part of the estuary near Rigolet. Broadening the survey area would help to better quantify the impact of Atlantic water intrusion on the biodiversity and distribution of fish within the estuary, especially given the very dynamics currents in the region (Durkalec et al. 2016; Kamula et al. 2017).

This study provides baseline information on habitat, diversity, and distribution of pelagic fish in Lake Melville prior to the operation of the second large scale hydroelectric project upstream. The information presented in this thesis can be used to build on the existing literature and local knowledge while providing insight for future water management practices within the Lake Melville system. The results also contribute to the growing body of knowledge on the impacts of producing renewable hydroelectric energy on estuarine ecosystems and emphasize the importance of long-term ecological monitoring practices, especially near Indigenous communities that rely on environmental resources.

References

Abraham, D.A. 2019a. Introduction to Underwater Acoustic Signal Processing. *In* Underwater Acoustic Signal Processing: Modeling, Detection, and Estimation. *Edited by* D.A. Abraham. Springer International Publishing, Cham. pp. 3–32. doi:10.1007/978-3-319-92983-5_1.

Abraham, D.A. 2019b. Underwater Acoustic Signal and Noise Modeling. *In* Underwater Acoustic Signal Processing: Modeling, Detection, and Estimation. *Edited by* D.A. Abraham. Springer International Publishing, Cham. pp. 349–456. doi:10.1007/978-3-319-92983-5_7.

Akenhead, S.A., and Bobbitt, J. 1986. The Capacity of Lake Melville Fjord to Store Runoff. *In* The Role of Freshwater Outflow in Coastal Marine Ecosystems. *Edited by* S. Skreslet. Springer, Berlin, Heidelberg. pp. 183–194. doi:10.1007/978-3-642-70886-2_11.

Anderson, M.R. 2011. Duration and extent of elevated mercury levels in downstream fish following reservoir creation. River Systems **19**(3): 167–176. doi:10.1127/1868-5749/2011/019-0023.

Backus, R.H. 1957. The Fishes of Labrador. Woods Hole Oceanographic Institution, Woods Hole, Massachusetts.

Baos, R., Cabezas, S., González, M.J., Jiménez, B., and Delibes, M. 2022. Eurasian otter (Lutra lutra) as sentinel species for the long-term biomonitoring of the Guadiamar River after the Aznalcóllar mine spill. Science of The Total Environment **802**: 149669. doi:10.1016/j.scitotenv.2021.149669.

Becker, A., Whitfield, A.K., Cowley, P.D., and Cole, V.J. 2017. Does water depth influence size composition of estuary-associated fish? Distributions revealed using mobile acoustic-camera transects along the channel of a small shallow estuary. Mar. Freshwater Res. **68**(11): 2163–2169. CSIRO PUBLISHING. doi:10.1071/MF16230.

Belyanina, T.N. 1969. Synopsis of biological data on smelt Osmerus eperlanus (Linnaeus) 1758. Food and Agriculture Organization of the United Nations Fisheries Synopsis.

Berger, C.S., Bougas, B., Turgeon, S., Ferchiou, S., Ménard, N., Bernatchez, L., . 2020. Groundtruthing of pelagic forage fish detected by hydroacoustics in a whale feeding area using environmental DNA. Environmental DNA **2**(4): 477–492. John Wiley & Sons, Inc., Hoboken, United States. doi:http://dx.doi.org/10.1002/edn3.73.

Blaber, S.J.M., and Blaber, T.G. 1980. Factors affecting the distribution of juvenile estuarine and inshore fish. Journal of Fish Biology **17**(2): 143–162. doi:10.1111/j.1095-8649.1980.tb02749.x.

Bobbitt, J. 1982. Influence of controlled discharge from the Churchill River on the oceanography of Groswater Bay, Labrador. Research and Resource Services, Deptof Fisheries and Oceans, St. John's.

Bonanno, G., and Orlando-Bonaca, M. 2017. Trace elements in Mediterranean seagrasses: Accumulation, tolerance and biomonitoring. A review. Marine Pollution Bulletin **125**(1): 8–18. doi:10.1016/j.marpolbul.2017.10.078.

Bouchard, C., and Fortier, L. 2008. Effects of polynyas on the hatching season, early growth and survival of polar cod Boreogadus saida in the Laptev Sea. Mar. Ecol. Prog. Ser. **355**: 247–256. doi:10.3354/meps07335.

Bouchard, C., and Fortier, L. 2011. Circum-arctic comparison of the hatching season of polar cod Boreogadus saida: A test of the freshwater winter refuge hypothesis. Progress in Oceanography **90**(1): 105–116. doi:10.1016/j.pocean.2011.02.008.

Bradbury, I., Campana, S., and Bentzen, P. 2008. Otolith elemental composition and adult tagging reveal spawning site fidelity and estuarine dependency in rainbow smelt. Mar. Ecol. Prog. Ser. **368**: 255–268. doi:10.3354/meps07583.

Bradbury, I.R., Campana, S.E., Bentzen, P., and Snelgrove, P.V.R. 2004. Synchronized hatch and its ecological significance in rainbow smelt Osmerus mordax in St. Mary's Bay, Newfoundland. Limnol. Oceanogr. **49**(6): 2310–2315. doi:10.4319/lo.2004.49.6.2310.

Bradbury, I.R., Gardiner, K., Snelgrove, P.V., Campana, S.E., Bentzen, P., and Guan, L. 2006. Larval transport, vertical distribution, and localized recruitment in anadromous rainbow smelt (Osmerus mordax). Canadian Journal of Fisheries & Aquatic Sciences **63**(12): 2822–2836. Canadian Science Publishing. doi:10.1139/f06-164.

Campuzano, F.J., Juliano, M., Sobrinho, J., dePablo, H., Brito, D., Fernandes, R., and Neves, R. 2017. Coupling Watersheds, Estuaries and Regional Oceanography through Numerical Modelling in the Western Iberia: Thermohaline Flux Variability at the Ocean-Estuary Interface. *In* Estuary. IntechOpen. doi:10.5772/intechopen.72162.

Canterbury, G.E., Martin, T.E., Petit, D.R., Petit, L.J., and Bradford, D.F. 2000. Bird Communities and Habitat as Ecological Indicators of Forest Condition in Regional Monitoring. Conservation Biology **14**(2): 544–558. doi:10.1046/j.1523-1739.2000.98235.x.

Carassou, L., Dzwonkowski, B., Hernandez, F.J., Powers, S.P., Park, K., Graham, W.M., and Mareska, J. 2011. Environmental Influences on Juvenile Fish Abundances in a River-Dominated Coastal System. Marine and Coastal Fisheries **3**(1): 411–427. Taylor & Francis. doi:10.1080/19425120.2011.642492.

Carignan, V., and Villard, M.-A. 2002. Selecting Indicator Species to Monitor Ecological Integrity: A Review. Environ Monit Assess **78**(1): 45–61. doi:10.1023/A:1016136723584.

Chatwin, P.C. 1976. Some remarks on the maintenance of the salinity distribution in estuaries. Estuarine and Coastal Marine Science **4**(5): 555–566. doi:10.1016/0302-3524(76)90030-X.

Chiles, J.-P., and Delfiner, P. 2012. Geostatistics modeling spatial uncertainty, second edition. *In* 2nd ed. John Wiley & Sons, Hoboken, N.J.

Clarke, K.D., Pratt, T.C., Smokorowski, K.E., Randall, R.G., and Scruton, D.A. 2008. Validation of the flow management pathway : effects of altered flow on fish habitat and fishes downstream from a hydropower dam. Available from https://www.osti.gov/etdeweb/biblio/21097065 [accessed 13 March 2022].

Costanza, R., d'Arge, R., de Groot, R., Farber, S., Grasso, M., Hannon, B., Limburg, K., Naeem, S., O'Neill, R.V., Paruelo, J., Raskin, R.G., Sutton, P., and van den Belt, M. 1998. The value of the world's ecosystem services and natural capital. Ecological Economics **25**(1): 3–15. doi:10.1016/S0921-8009(98)00020-2.

Cottier, F.R., Nilsen, F., Skogseth, R., Tverberg, V., Skarðhamar, J., and Svendsen, H. 2010. Arctic fjords: a review of the oceanographic environment and dominant physical processes. Geological Society, London, Special Publications **344**(1): 35–50. The Geological Society of London. doi:10.1144/SP344.4.

Coutant, C.C., and Whitney, R.R. 2000. Fish Behavior in Relation to Passage through Hydropower Turbines: A Review. Transactions of the American Fisheries Society **129**(2): 351–380. Taylor & Francis. doi:10.1577/1548-8659(2000)129<0351:FBIRTP>2.0.CO;2.

Cushing, D.H. 1990. Plankton Production and Year-class Strength in Fish Populations: an Update of the Match/Mismatch Hypothesis. Advances in Marine Biology **26**: 249–293. Academic Press. doi:10.1016/S0065-2881(08)60202-3.

Cyr, F., S. Snook, C. Bishop, P.S. Galbraith, N. Chen and G. Han. 2022. Physical Oceanographic Conditions on the Newfoundland and Labrador Shelf during 2021. DFO Can. Sci. Advis. Sec. Res. Doc. 2022/040. iv + 48 p.

Dadswell, M.J., Spares, A.D., Mclean, M.F., Harris, P.J., and Rulifson, R.A. 2018. Long-term effect of a tidal, hydroelectric propeller turbine on the populations of three anadromous fish species. Journal of Fish Biology **93**(2): 192–206. doi:10.1111/jfb.13755.

De Robertis, A., and Higginbottom, I. 2007. A post-processing technique to estimate the signal-to-noise ratio and remove echosounder background noise. ICES Journal of Marine Science **64**(6): 1282–1291. doi:10.1093/icesjms/fsm112.

Deiner, K., and Altermatt, F. 2014. Transport Distance of Invertebrate Environmental DNA in a Natural River. PLOS ONE **9**(2): e88786. doi:10.1371/journal.pone.0088786.

Dejean, T., Valentini, A., Duparc, A., Pellier-Cuit, S., Pompanon, F., Taberlet, P., and Miaud, C. 2011. Persistence of Environmental DNA in Freshwater Ecosystems. PLoS ONE **6**(8): e23398. doi:10.1371/journal.pone.0023398.

Demer, D.A., Berger, L., Bernasconi, M., Bethke, E., Boswell, K., Chu, D., Domokos, R., Dunford, A., Fassler, S., Gauthier, S., Hufnagle, L.T., Jech, J.M., Bouffant, N., Lebourges-Dhaussy, A., Lurton, X., Macaulay, G.J., Perrot, Y., Ryan, T., Parker-Stetter, S., Stienessen, S., Weber, T., and Williamson, N. 2015. Calibration of acoustic instruments. Report, International Council for the Exploration of the Sea (ICES). doi:http://dx.doi.org/10.25607/OBP-185.

Dijkstra, Y.M., and Schuttelaars, H.M. 2020. A Unifying Approach to Subtidal Salt Intrusion Modeling in Tidal Estuaries. Journal of Physical Oceanography **51**(1): 147–167. American Meteorological Society. doi:10.1175/JPO-D-20-0006.1.

Dijkstra, Y.M., and Schuttelaars, H.M. 2021. Adjustment and Extension of the Hansen and Rattray Estuarine Classification Diagram. Journal of Physical Oceanography **51**(9): 2903–2913. American Meteorological Society. doi:10.1175/JPO-D-21-0021.1.

Durkalec, A., Sheldon, T., and Bell, T. 2016. Lake Melville: Avativut Kanuittailinnivut (Our Environment, Our Health) Scientific Report. Nunatsiavut Government, Nain, NL.

Easson, C.G., Boswell, K.M., Tucker, N., Warren, J.D., and Lopez, J.V. 2020. Combined eDNA and Acoustic Analysis Reflects Diel Vertical Migration of Mixed Consortia in the Gulf of Mexico. Frontiers in Marine Science. Frontiers Research Foundation, Lausanne, Switzerland. doi:http://dx.doi.org/10.3389/fmars.2020.00552.

Evans, N.T., Li, Y., Renshaw, M.A., Olds, B.P., Deiner, K., Turner, C.R., Jerde, C.L., Lodge, D.M., Lamberti, G.A., and Pfrender, M.E. 2017. Fish community assessment with eDNA metabarcoding: effects of sampling design and bioinformatic filtering. Can. J. Fish. Aquat. Sci. **74**(9): 1362–1374. NRC Research Press. doi:10.1139/cjfas-2016-0306.

Farmer, D.M., and Freeland, H.J. 1983. The physical oceanography of Fjords. Progress in Oceanography **12**(2): 147–219. doi:10.1016/0079-6611(83)90004-6.

Ferreira, M., Antunes, P., Gil, O., Vale, C., and Reis-Henriques, M.A. 2004. Organochlorine contaminants in flounder (Platichthys flesus) and mullet (Mugil cephalus) from Douro estuary, and their use as sentinel species for environmental monitoring. Aquatic Toxicology **69**(4): 347–357. doi:10.1016/j.aquatox.2004.06.005.

França, S., and Cabral, H.N. 2016. Predicting fish species distribution in estuaries: Influence of species' ecology in model accuracy. Estuarine, Coastal and Shelf Science **180**: 11–20. doi:10.1016/j.ecss.2016.06.010.

Fuji, T., Kasai, A., Suzuki, K.W., Ueno, M., and Yamashita, Y. 2010. Freshwater migration and feeding habits of juvenile temperate seabass Lateolabrax japonicus in the stratified Yura River estuary, the Sea of Japan. Fisheries Science **76**(4): 643–652. Springer Nature B.V., Tokyo, Netherlands. doi:http://dx.doi.org.qe2a-proxy.mun.ca/10.1007/s12562-010-0258-y.

Geoffroy, M., Majewski, A., LeBlanc, M., Gauthier, S., Walkusz, W., Reist, J., and Fortier, L. 2016. Vertical segregation of age-0 and age-1+ polar cod (Boreogadus saida) over the annual cycle in the Canadian Beaufort Sea. Polar Biology **39**. doi:10.1007/s00300-015-1811-z.

Georgakarakos, S., and Kitsiou, D. 2008. Mapping abundance distribution of small pelagic species applying hydroacoustics and Co-Kriging techniques. Hydrobiologia **612**(1): 155–169. doi:10.1007/s10750-008-9484-z.

Goldberg, C.S., Pilliod, D.S., Arkle, R.S., and Waits, L.P. 2011. Molecular Detection of Vertebrates in Stream Water: A Demonstration Using Rocky Mountain Tailed Frogs and Idaho Giant Salamanders. PLOS ONE **6**(7): e22746. Public Library of Science. doi:10.1371/journal.pone.0022746.

Grote, B., Stenevik, E., Ekau, W., Verheye, H., Lipiński, M., and Hagen, W. 2012. Spawning strategies and transport of early stages of the two Cape hake species, Merluccius paradoxus and M. capensis , in the southern Benguela upwelling system. African Journal of Marine Science **34**(2): 195–204. Taylor & Francis Ltd. doi:10.2989/1814232X.2012.675040.

Hallam, J., Clare, E.L., Jones, J.I., and Day, J.J. 2021. Biodiversity assessment across a dynamic riverine system: A comparison of eDNA metabarcoding versus traditional fish surveying methods. Environmental DNA **3**(6): 1247–1266. doi:10.1002/edn3.241.

Hamley, J.M. 1975. Review of Gillnet Selectivity. J. Fish. Res. Bd. Can. **32**(11): 1943–1969. NRC Research Press. doi:10.1139/f75-233.

Hansen, D.V., and Rattray Jr., M. 1966. New Dimensions in Estuary Classification1. Limnology and Oceanography **11**(3): 319–326. doi:10.4319/lo.1966.11.3.0319.

Head, E.J.H., Harris, L.R., and Yashayaev, I. 2003. Distributions of Calanus spp. and other mesozooplankton in the Labrador Sea in relation to hydrography in spring and summer (1995–2000). Progress in Oceanography **59**(1): 1–30. doi:10.1016/S0079-6611(03)00111-3.

Iles, T.D., and Sinclair, M. 1982. Atlantic Herring: Stock Discreteness and Abundance. Science **215**(4533): 627–633. American Association for the Advancement of Science.

Iwasaki, W., Fukunaga, T., Isagozawa, R., Yamada, K., Maeda, Y., Satoh, T.P., Sado, T., Mabuchi, K., Takeshima, H., Miya, M., and Nishida, M. 2013. MitoFish and MitoAnnotator: A Mitochondrial Genome Database of Fish with an Accurate and Automatic Annotation

Pipeline. Molecular Biology and Evolution **30**(11): 2531–2540. doi:10.1093/molbev/mst141.

Kamula, C.M., Kuzyk, Z.Z.A., Lobb, D.A., and Macdonald, R.W. 2017. Sources and accumulation of sediment and particulate organic carbon in a subarctic fjard estuary: ^{210}Pb, ^{137}Cs, and δ^{13}C records from Lake Melville, Labrador. Can. J. Earth Sci. **54**(9): 993–1006. doi:10.1139/cjes-2016-0167.

Lacoursière-Roussel, A., Howland, K., Normandeau, E., Grey, E.K., Archambault, P., Deiner, K., Lodge, D.M., Hernandez, C., Leduc, N., and Bernatchez, L. 2018. eDNA metabarcoding as a new surveillance approach for coastal Arctic biodiversity. Ecology and Evolution **8**(16): 7763–7777. John Wiley & Sons, Inc., Bognor Regis, United States. doi:10.1002/ece3.4213.

Leggett, W.C., and Deblois, E. 1994. Recruitment in marine fishes: Is it regulated by starvation and predation in the egg and larval stages? Netherlands Journal of Sea Research **32**(2): 119–134. doi:10.1016/0077-7579(94)90036-1.

Liu, X., Qin, J., Xu, Y., Zhou, M., Wu, X., and Ouyang, S. 2019a. Biodiversity pattern of fish assemblages in Poyang Lake Basin: Threat and conservation. Ecology and Evolution **9**(20): 11672–11683. John Wiley & Sons, Inc., Bognor Regis, United States. doi:http://dx.doi.org/10.1002/ece3.5661.

Liu, X., Qin, J., Xu, Y., Ouyang, S., and Wu, X. 2019b. Biodiversity decline of fish assemblages after the impoundment of the Three Gorges Dam in the Yangtze River Basin, China. Rev Fish Biol Fisheries **29**(1): 177–195. doi:10.1007/s11160-019-09548-0.

Lodge, D.M., Turner, C.R., Jerde, C.L., Barnes, M.A., Chadderton, L., Egan, S.P., Feder, J.L., Mahon, A.R., and Pfrender, M.E. 2012. Conservation in a cup of water: estimating biodiversity and population abundance from environmental DNA. Molecular Ecology **21**(11): 2555–2558. doi:10.1111/j.1365-294X.2012.05600.x.

Love, R. H. (1971). Measurements of fish target strength: a review. Fish. Bull, **69**(4), 703-715.

Lu, Z., DeYoung, B., and Foley, J. 2013. Analysis of Physical Oceanographic Data from Lake Melville, Labrador, July - September 2012. Physics and Physical Oceanography Data Report, Department of Physics and Physical Oceanography Memorial University of Newfoundland, St. John's, NL.

MacLennan, D.N., and Simmonds, E.J. 2013. Fisheries Acoustics. Springer Science & Business Media.

Mauvisseau, Q., Coignet, A., Delaunay, C., Pinet, F., Bouchon, D., and Souty-Grosset, C. 2018. Environmental DNA as an efficient tool for detecting invasive crayfishes in freshwater ponds. Hydrobiologia **805**(1): 163–175. Springer Nature. doi:10.1007/s10750-017-3288-y.

McCarthy, J.H., and Gosse, M. 2015. Aquatic Environmental Effects Monitoring Program 1998 to 2014 Baseline Conditions Muskrat Falls. Amec Foster Wheeler Environment & Infrastructure.

McCarthy, J.H., and Gosse, M. 2018. Aquatic Species Habitat Utilization Overview. Churchill River, Goose Bay, and Lake Melville 1998-2016.

McClatchie, S., Thorne, R.E., Grimes, P., and Hanchet, S. 2000. Ground truth and target identification for fisheries acoustics. Fisheries Research **47**(2): 173–191. doi:10.1016/S0165-7836(00)00168-5.

McDougall, T., and Barker, P. 2011. Getting started with TEOS-10 and the Gibbs Seawater (GSW) Oceanographic Toolbox. SCOR/IAPSO WG127. Available from https://www.teos-10.org/pubs/Getting_Started.pdf [accessed 15 April 2023].

Meerhoff, E., Castro, L., and Tapia, F. 2013. Influence of freshwater discharges and tides on the abundance and distribution of larval and juvenile Munida gregaria in the Baker river estuary, Chilean Patagonia. Continental Shelf Research **61–62**: 1–11. doi:10.1016/j.csr.2013.04.025.

Mello, L.G.S., and Rose, G.A. 2009. The acoustic dead zone: theoretical vs. empirical estimates, and its effect on density measurements of semi-demersal fish. ICES Journal of Marine Science **66**(6): 1364–1369. doi:10.1093/icesjms/fsp099.

Miya, M., Sato, Y., Fukunaga, T., Sado, T., Poulsen, J.Y., Sato, K., Minamoto, T., Yamamoto, S., Yamanaka, H., Araki, H., Kondoh, M., and Iwasaki, W. 2015. MiFish, a set of universal PCR primers for metabarcoding environmental DNA from fishes: detection of more than 230 subtropical marine species. Royal Society Open Science **2**(7): 150088. Royal Society. doi:10.1098/rsos.150088.

Montagna, P.A., Palmer, T.A., and Beseres Pollack, J. 2013. Hydrological Changes and Estuarine Dynamics. Springer New York, New York, NY. doi:10.1007/978-1-4614-5833-3.

Murawski, S.A., Clayton, G.R., Reed, R.J., and Cole, C.F. 1980. Movements of Spawning Rainbow Smelt, Osmerus mordax, in a Massachusetts Estuary. Estuaries **3**(4): 308–314. doi:10.2307/1352086.

North, E., and Houde, E. 2003. Linking ETM physics, zooplankton prey, and fish early-life histories to striped bass Morone saxatilis and white perch M. americana recruitment. Mar. Ecol. Prog. Ser. **260**: 219–236. doi:10.3354/meps260219.

Ona, E., and Mitson, R.B. 1996. Acoustic sampling and signal processing near the seabed: the deadzone revisited. ICES Journal of Marine Science **53**(4): 677–690. doi:10.1006/jmsc.1996.0087.

Parker-Stetter, S.L., Rudstam, L.G., Sullivan, P.J., and Warner, D.M. 2009. Standard operating procedures for fisheries acoustic surveys in the Great Lakes. Special publication, Great Lakes Fishery Commission, Ann Arbor, MI.

Paterson, A.W., and Whitfield, A.K. 2000. Do Shallow-water Habitats Function as Refugia for Juvenile Fishes? Estuarine, Coastal and Shelf Science **51**(3): 359–364. doi:10.1006/ecss.2000.0640.

Pebesma, E., J. 2004. Multivariable geostatistics in S: the gstat package. Computers & Geosciences **30**: 683–691.

Pepin, P. 2013. Distribution and feeding of Benthosema glaciale in the western Labrador Sea: Fish–zooplankton interaction and the consequence to calanoid copepod populations. Deep Sea Research Part I: Oceanographic Research Papers **75**: 119–134. doi:10.1016/j.dsr.2013.01.012.

Pepin, P., Robert, D., Bouchard, C., Dower, J.F., Falardeau, M., Fortier, L., Jenkins, G.P., Leclerc, V., Levesque, K., Llopiz, J.K., Meekan, M.G., Murphy, H.M., Ringuette, M., Sirois, P., and Sponaugle, S. 2015. Once upon a larva: revisiting the relationship between feeding success and growth in fish larvae. ICES Journal of Marine Science **72**(2): 359–373. doi:10.1093/icesjms/fsu201.

Pérez-Santos, I., Castro, L., Ross, L., Niklitschek, E., Mayorga, N., Cubillos, L., Gutierrez, M., Escalona, E., Castillo, M., Alegría, N., and Daneri, G. 2018. Turbulence and hypoxia contribute to dense biological scattering layers in a Patagonian fjord system. Ocean Science **14**(5): 1185–1206. Copernicus GmbH, Katlenburg-Lindau, Germany. doi:10.5194/os-14-1185-2018.

Peterson, R.C., Jennings, C.A., and Peterson, J.T. 2013. Relationships Between River Discharge and Abundance of Age 0 Redhorses (moxostoma Spp.) in the Oconee River, Georgia, Usa, with Implications for Robust Redhorse. River Research and Applications **29**(6): 734–742. doi:10.1002/rra.2566.

Petitgas, P., Woillez, M., Renard, D., Bez, N., and Rivoirard, J. 2017. Handbook of Geostatistics in R for Fisheries and Marine Ecology. ICES. doi:10.17895/ICES.PUB.3717.

Pippy, B.A., Kidd, K.A., Munkittrick, K.R., Mercer, A., and Hunt, H. 2016. Use of the Atlantic nut clam (Nucula proxima) and catworm (Nephtys incisa) in a sentinel species approach for monitoring the health of Bay of Fundy estuaries. Marine Pollution Bulletin **106**(1): 225–235. doi:10.1016/j.marpolbul.2016.02.065.

Poff, N.L., Allan, J.D., Bain, M.B., Karr, J.R., Prestegaard, K.L., Richter, B.D., Sparks, R.E., and Stromberg, J.C. 1997. The Natural Flow Regime. BioScience **47**(11): 769–784. doi:10.2307/1313099.

Renöfält, B.M., Jansson, R., and Nilsson, C. 2010. Effects of hydropower generation and opportunities for environmental flow management in Swedish riverine ecosystems. Freshwater Biology **55**(1): 49–67. doi:10.1111/j.1365-2427.2009.02241.x.

Rooyen, A. van, Miller, A.D., Clark, Z., Sherman, C.D.H., Butcher, P.A., Rizzari, J.R., and Weeks, A.R. 2021. Development of an environmental DNA assay for detecting multiple shark species involved in human–shark conflicts in Australia. Environmental DNA **3**(5): 940–949. John Wiley & Sons, Inc., Hoboken, United States. doi:http://dx.doi.org.qe2a-proxy.mun.ca/10.1002/edn3.202.

Röpke, A., Nellent, W., and Piatkowski, U. 1993. A comparative study on the influence of the pycnocline on the vertical distribution of fish larvae and cephalopod paralarvae in three ecoligically different areas of the Arabian Sea. Deep Sea Research Part II: Topical Studies in Oceanography **40**(3): 801–819. doi:10.1016/0967-0645(93)90059-V.

Roswell, M., Dushoff, J., and Winfree, R. 2021. A conceptual guide to measuring species diversity. Oikos **130**(3): 321–338. doi:10.1111/oik.07202.

Rudstam, L.G., Parker, S.L., Einhouse, D.W., Witzel, L.D., Warner, D.M., Stritzel, J.L., Parrish, D.L., and Sullivan, P.J. 2003. Application of in situ target-strength estimations in lakes: examples from rainbow-smelt surveys in Lakes Erie and Champlain. ICES Journal of Marine Science **60**(3): 500–507. doi:10.1016/S1054-3139(03)00046-8.

Rudstam, L.G., Parker-Stetter, S.L., Sullivan, P.J., and Warner, D.M. 2009. Towards a standard operating procedure for fishery acoustic surveys in the Laurentian Great Lakes, North America. ICES J Mar Sci **66**(6): 1391–1397. doi:10.1093/icesjms/fsp014.

Ryan, T.E., Downie, R.A., Kloser, R.J., and Keith, G. 2015. Reducing bias due to noise and attenuation in open-ocean echo integration data. ICES Journal of Marine Science **72**(8): 2482–2493. doi:10.1093/icesjms/fsv121.

Rytwinski, T., Harper, M., Taylor, J.J., Bennett, J.R., Donaldson, L.A., Smokorowski, K.E., Clarke, K., Bradford, M.J., Ghamry, H., Olden, J.D., Boisclair, D., and Cooke, S.J. 2020. What are

the effects of flow-regime changes on fish productivity in temperate regions? A systematic map. Environmental Evidence **9**(1): 7. doi:10.1186/s13750-020-00190-z.

Salgado, L.D., Marques, A.E.M.L., Kramer, R.D., Oliveira, F.G. de, Moretto, S.L., Lima, B.A. de, Prodocimo, M.M., Cestari, M.M., Azevedo, J.C.R. de, and Silva de Assis, H.C. 2019. Integrated assessment of sediment contaminant levels and biological responses in sentinel fish species Atherinella brasiliensis from a sub-tropical estuary in south Atlantic. Chemosphere **219**: 15–27. doi:10.1016/j.chemosphere.2018.11.204.

Sánchez-Velasco, L., Lavín, M.F., Jiménez-Rosenberg, S.P.A., Montes, J.M., and Turk-Boyer, P.J. 2012. Larval fish habitats and hydrography in the Biosphere Reserve of the Upper Gulf of California (June 2008). Continental Shelf Research **33**: 89–99. doi:10.1016/j.csr.2011.11.009.

Saucier, F. J., Roy, F., Senneville, S., Smith, G., Lefaivre, D., Zakardjian, B., & Dumais, J. F. (2009). Modélisation de la circulation dans l'estuaire et le golfe du Saint-Laurent en réponse aux variations du débit d'eau douce et des vents. Revue des Sciences de l'Eau, **22**(2), 159-176.

Schartup, A.T., Balcom, P.H., Soerensen, A.L., Gosnell, K.J., Calder, R.S.D., Mason, R.P., and Sunderland, E.M. 2015. Freshwater discharges drive high levels of methylmercury in Arctic marine biota. Proc. Natl. Acad. Sci. U.S.A. **112**(38): 11789–11794. doi:10.1073/pnas.1505541112.

Scopel, L.C., Diamond, A.W., Kress, S.W., Hards, A.R., and Shannon, P. 2018. Seabird diets as bioindicators of Atlantic herring recruitment and stock size: a new tool for ecosystem-based fisheries management. Can. J. Fish. Aquat. Sci. **75**(8): 1215–1229. NRC Research Press. doi:10.1139/cjfas-2017-0140.

Shannon, C.E. 1948. A mathematical theory of communication. The Bell System Technical Journal **27**(3): 379–423. doi:10.1002/j.1538-7305.1948.tb01338.x.

Simard, Y., Lavoie, D., and Saucier, F.J. 2002. Channel head dynamics: Capelin (Mallotus villosus) aggregation in the tidally driven upwelling system of the Saguenay - St. Lawrence Marine Park's whale feeding ground. Canadian Journal of Fisheries and Aquatic Sciences **59**(2): 197–210. Canadian Science Publishing NRC Research Press, Ottawa, Canada.

Simmonds, E.J. 2005. Fisheries acoustics: theory and practice. *In* 2nd ed.. Blackwell Science, Oxford ; Ames, Iowa.

Simmonds, J., and MacLennan, D.N. 2008. Fisheries Acoustics: Theory and Practice. John Wiley & Sons.

Simo-Matchim, A.-G., Gosselin, M., Blais, M., Gratton, Y., and Tremblay, J.-É. 2016. Seasonal variations of phytoplankton dynamics in Nunatsiavut fjords (Labrador, Canada) and their relationships with environmental conditions. Journal of Marine Systems **156**: 56–75. doi:10.1016/j.jmarsys.2015.11.007.

Simpson, E. 1949. Measurement of Diversity. Nature **163**(4148): 688–688. Macmillan Magazines Ltd, London. doi:10.1038/163688a0.

Sirois, P., Lecomte, F., and Dodson, J.J. 1998. An otolith-based back-calculation method to account for time-varying growth rate in rainbow smelt (Osmerus mordax) larvae. Canadian Journal of Fisheries and Aquatic Sciences **55**(12): 2662–2671. Canadian Science Publishing NRC Research Press, Ottawa, Canada.

Spens, J., Evans, A.R., Halfmaerten, D., Knudsen, S.W., Sengupta, M.E., Mak, S.S.T., Sigsgaard, E.E., and Hellström, M. 2017. Comparison of capture and storage methods for aqueous macrobial eDNA using an optimized extraction protocol: advantage of enclosed filter. Methods in Ecology and Evolution **8**(5): 635–645. doi:10.1111/2041-210X.12683.

Stanton, T.K., Sellers, C.J., and Jech, J.M. 2012. Resonance classification of mixed assemblages of fish with swimbladders using a modified commercial broadband acoustic echosounder at 1-6 kHz. Canadian Journal of Fisheries & Aquatic Sciences **69**(5): 854–868. Canadian Science Publishing. doi:10.1139/f2012-013.

Stoeckle, M.Y., Soboleva, L., and Charlop-Powers, Z. 2017. Aquatic environmental DNA detects seasonal fish abundance and habitat preference in an urban estuary. PloS one **12**(4): e0175186. doi:http://dx.doi.org.qe2a-proxy.mun.ca/10.1371/journal.pone.0175186.

Stritzel Thomson, J.L., Parrish, D.L., Parker-Stetter, S.L., Rudstam, L.G., and Sullivan, P.J. 2011. Growth rates of rainbow smelt in Lake Champlain: effects of density and diet. Ecology of Freshwater Fish **20**(4): 503–512. doi:10.1111/j.1600-0633.2010.00472.x.

Sundby, S. 1990. Factors affecting the vertical distribution of eggs [HELP 34]. Havforskningsinstituttet. Available from https://imr.brage.unit.no/imr-xmlui/handle/11250/115253 [accessed 9 April 2022].

Sundby, S., and Kristiansen, T. 2015. The Principles of Buoyancy in Marine Fish Eggs and Their Vertical Distributions across the World Oceans. PLoS ONE **10**(10): 1–23. Public Library of Science. doi:10.1371/journal.pone.0138821.

Sutton, J. 2022, April. Phenology and growth of rainbow smelt (Osmerus mordax) in Lake Melville, Labrador, under increasing pressure from climate change and anthropogenic activities. masters, Memorial University of Newfoundland. Available from https://research.library.mun.ca/15461/ [accessed 13 January 2023].

Sylvester, E.V.A., Beiko, R.G., Bentzen, P., Paterson, I., Horne, J.B., Watson, B., Lehnert, S., Duffy, S., Clément, M., Robertson, M.J., and Bradbury, I.R. 2018. Environmental extremes drive population structure at the northern range limit of Atlantic salmon in North America. Molecular Ecology **27**(20): 4026–4040. doi:10.1111/mec.14849.

Taberlet, P., Coissac, E., Hajibabaei, M., and Rieseberg, L.H. 2012. Environmental DNA. Molecular Ecology **21**(8): 1789–1793. doi:10.1111/j.1365-294X.2012.05542.x.

Thompson, C.H., and Love, R.H. 1996. Determination of fish size distributions and areal densities using broadband low-frequency measurements. ICES Journal of Marine Science **53**(2): 197–201. doi:10.1006/jmsc.1996.0022.

Thomsen, P.F., Kielgast, J., Iversen, L.L., Wiuf, C., Rasmussen, M., Gilbert, M.T.P., Orlando, L., and Willerslev, E. 2012. Monitoring endangered freshwater biodiversity using environmental DNA. Molecular Ecology **21**(11): 2565–2573. doi:10.1111/j.1365-294X.2011.05418.x.

Turgeon, K., Turpin, C., and Gregory-Eaves, I. 2019. Dams have varying impacts on fish communities across latitudes: a quantitative synthesis. Ecology Letters **22**(9): 1501–1516. doi:10.1111/ele.13283.

Tverberg, V., Skogseth, R., Cottier, F., Sundfjord, A., Walczowski, W., Inall, M.E., Falck, E., Pavlova, O., and Nilsen, F. 2019. The Kongsfjorden Transect: Seasonal and Inter-annual Variability in Hydrography. *In* The Ecosystem of Kongsfjorden, Svalbard. *Edited by* H. Hop

and C. Wiencke. Springer International Publishing, Cham. pp. 49–104. doi:10.1007/978-3-319-46425-1_3.

Tzeng, W.-N., and Wang, Y.-T. 1993. Hydrography and distribution dynamics of larval and juvenile fishes in the coastal waters of the Tanshui River estuary, Taiwan, with reference to estuarine larval transport. Marine Biology **116**(2): 205–217. doi:10.1007/BF00350010.

Wells, N.J., Stenson, G.B., Pepin, P., and Koen-Alonso, M. (n.d.). Identification and Descriptions of Ecologically and Biologically Significant Areas in the Newfoundland and Labrador Shelves Bioregion. : 92.

Wu, H., Chen, J., Xu, J., Zeng, G., Sang, L., Liu, Q., Yin, Z., Dai, J., Yin, D., Liang, J., and Ye, S. 2019. Effects of dam construction on biodiversity: A review. Journal of Cleaner Production **221**: 480–489. doi:10.1016/j.jclepro.2019.03.001.

Wu, J., Huang, J., Han, X., Xie, Z., and Gao, X. 2003. Three-Gorges dam--experiment in habitat fragmentation? Science **300**(5623): 1239–40. The American Association for the Advancement of Science, Washington, United States.

Zou, K., Chen, J., Ruan, H., Li, Z., Guo, W., Li, M., and Liu, L. 2020. eDNA metabarcoding as a promising conservation tool for monitoring fish diversity in a coastal wetland of the Pearl River Estuary compared to bottom trawling. Science of The Total Environment **702**: 134704. doi:10.1016/j.scitotenv.2019.134704.

Figures

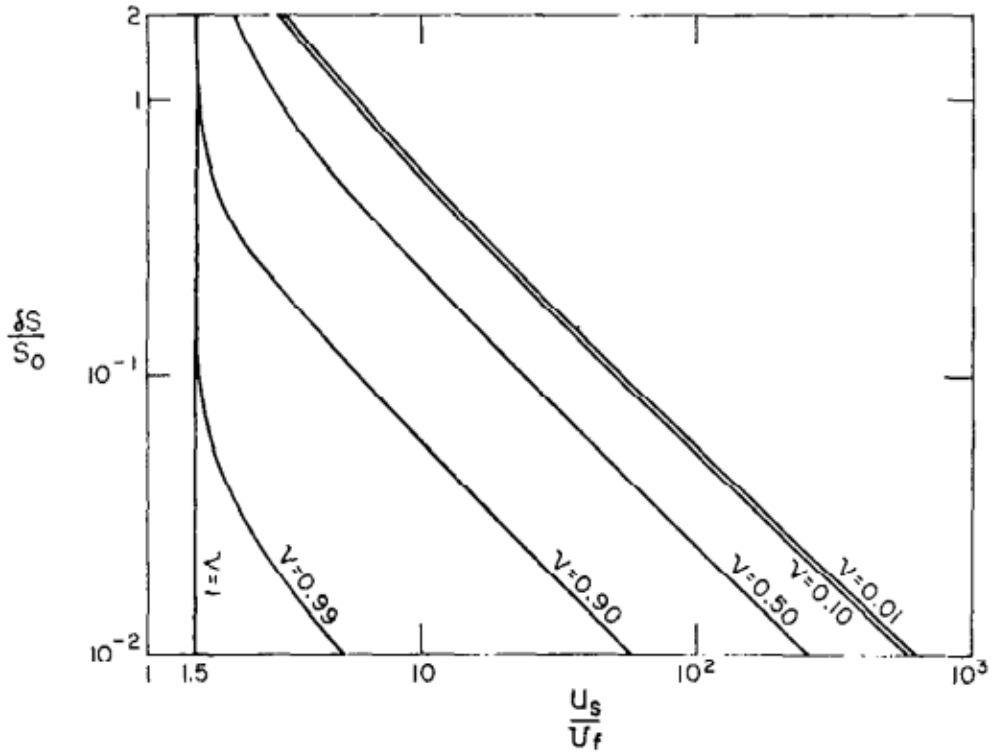

Figure 1. Stratification-circulation diagram from Hansen and Rattray (1996). Fraction of horizontal salt balance by diffusion, $\frac{\delta S}{S_0}$ represents the stratification parameter and $\frac{U_S}{U_f}$ represents the circulation parameter. When the diffusive fraction (ν) equals 1, gravitational convection ceases, and diffusion is entirely responsible for the upstream salt flux. As $\nu \rightarrow 0$ diffusion becomes less significant, and the upstream salt flux is caused by gravitational convection.

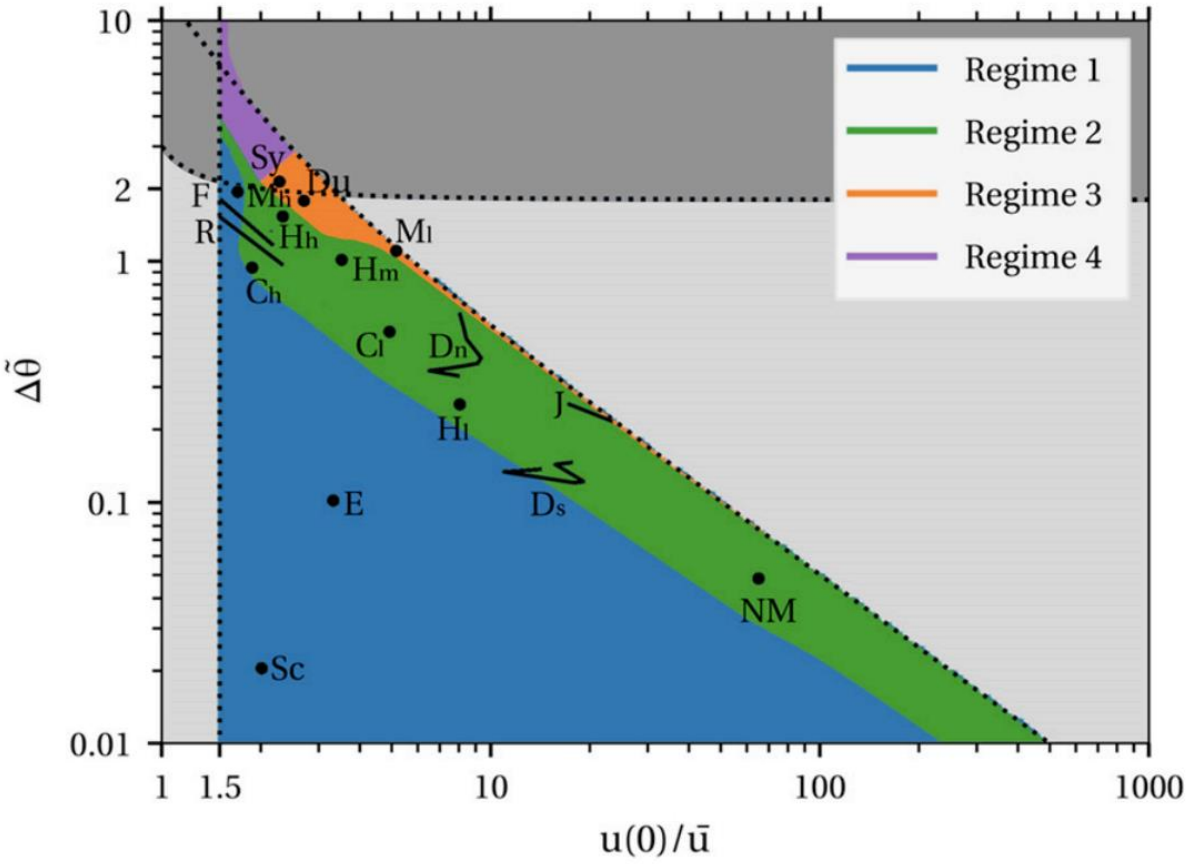

Figure 2. Expanded applications based on Hansen and Rattray (1966) (Figure 1) of the adjusted and extended classification diagram based on the regimes of (Dijkstra and Schuttelaars 2020) taken from Dijkstra and Schuttelaars (2021). Estuaries are denoted by black dots, lines denote along-channel stretch of the estuary. The letters indicate: C: Columbia (United States), D: Delaware (United States), Du: Duwamish (United States), E: Ems (Germany), F: Fraser (Canada), H: Hudson (United States), J: James (United States) M: Mississippi (United States), NM: Mersey Narrows (United Kingdom), R: Rotterdam Waterway (branch of the Rhine-Meuse delta, Netherlands), Sc: Scheldt (Belgium, Netherlands), Sy: Strymon (Greece). Subscripts l, m, and h denote low, moderate, and high river discharge. Grey spaces indicated unpermitted or physically unrealistic solutions.

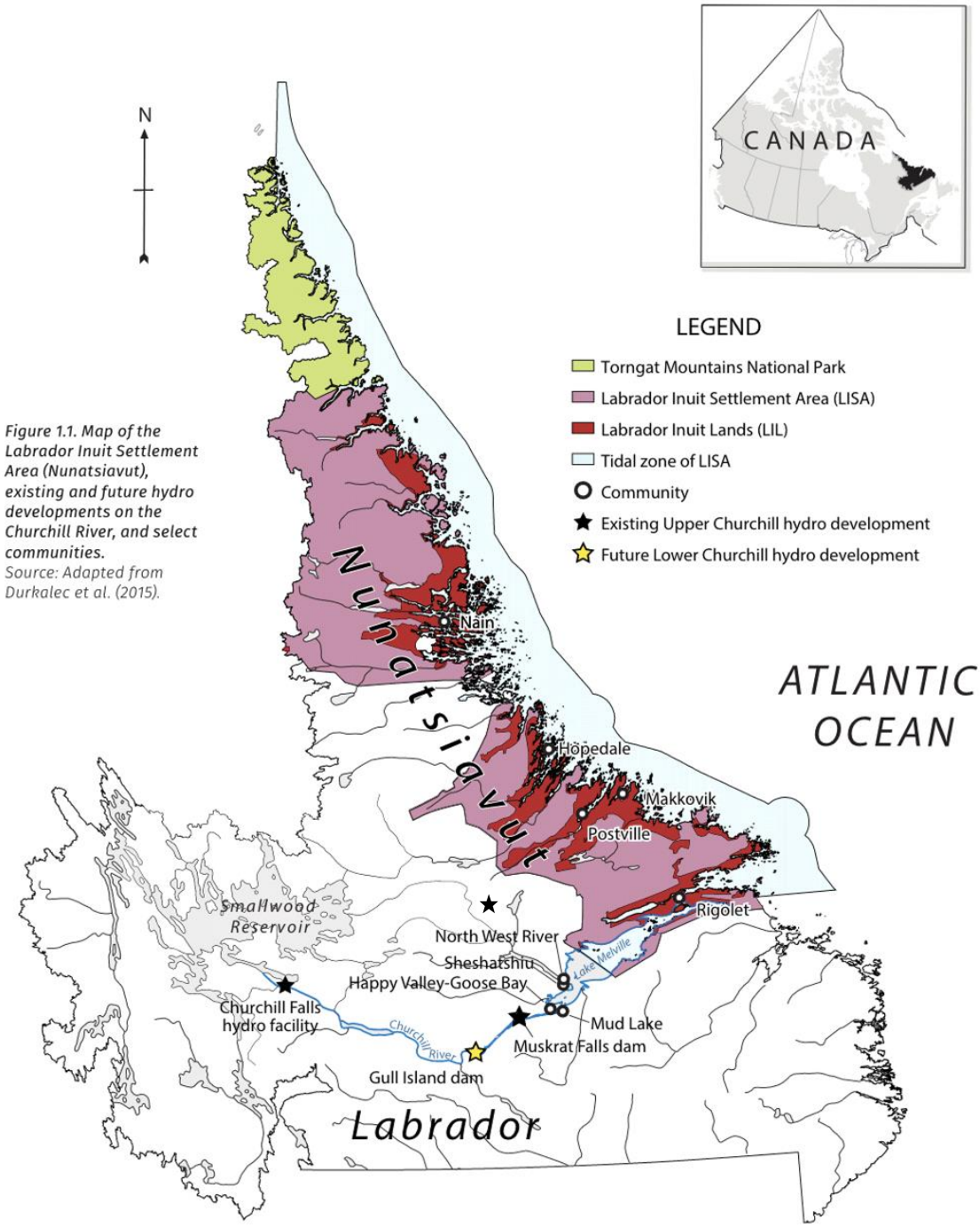

Figure 3. Map of Labrador from Durkalec et al. (2016) showing Nunatsiavut "Our Beautiful Land" and the Lake Melville System including the locations of the Churchill Falls Dam and Muskrat Falls Dam (yellow stars).

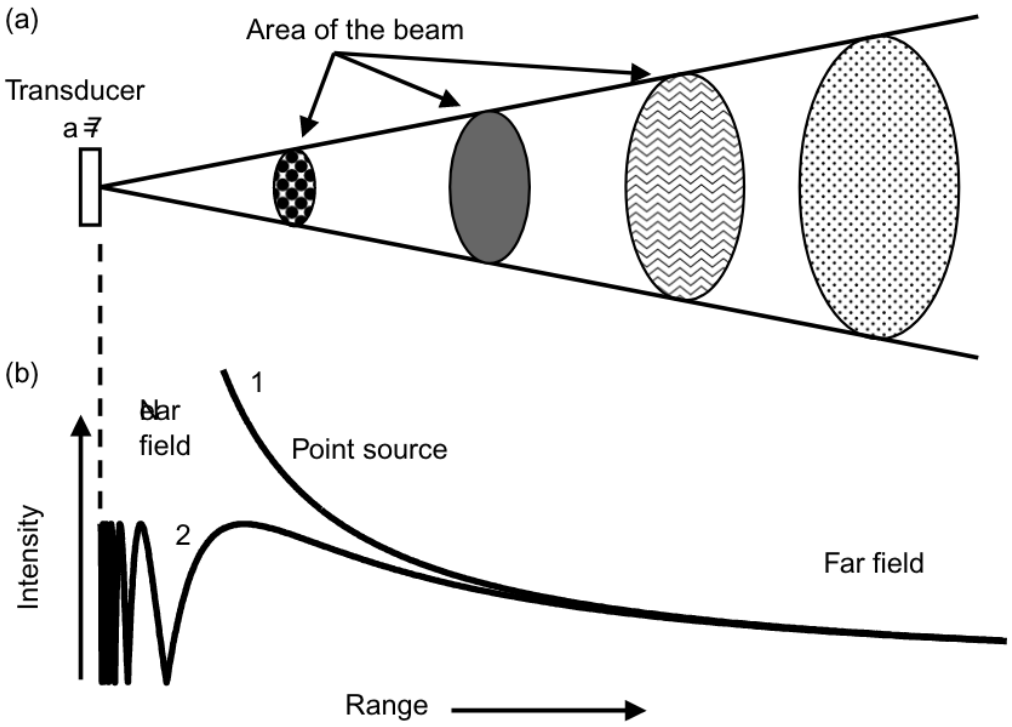

Figure 4. Schematic from MacLennan and Simmonds (2013) illustrating the acoustic energy propagating outwards from the transducer (size of 7°). (a) Spherical spreading showing that the intensity reduces as range increases. (b) This causes the intensity of the point source to follow the inverse-square law (curve 1). Near-field effect then limits the intensity close to the transducer face (curve 2).

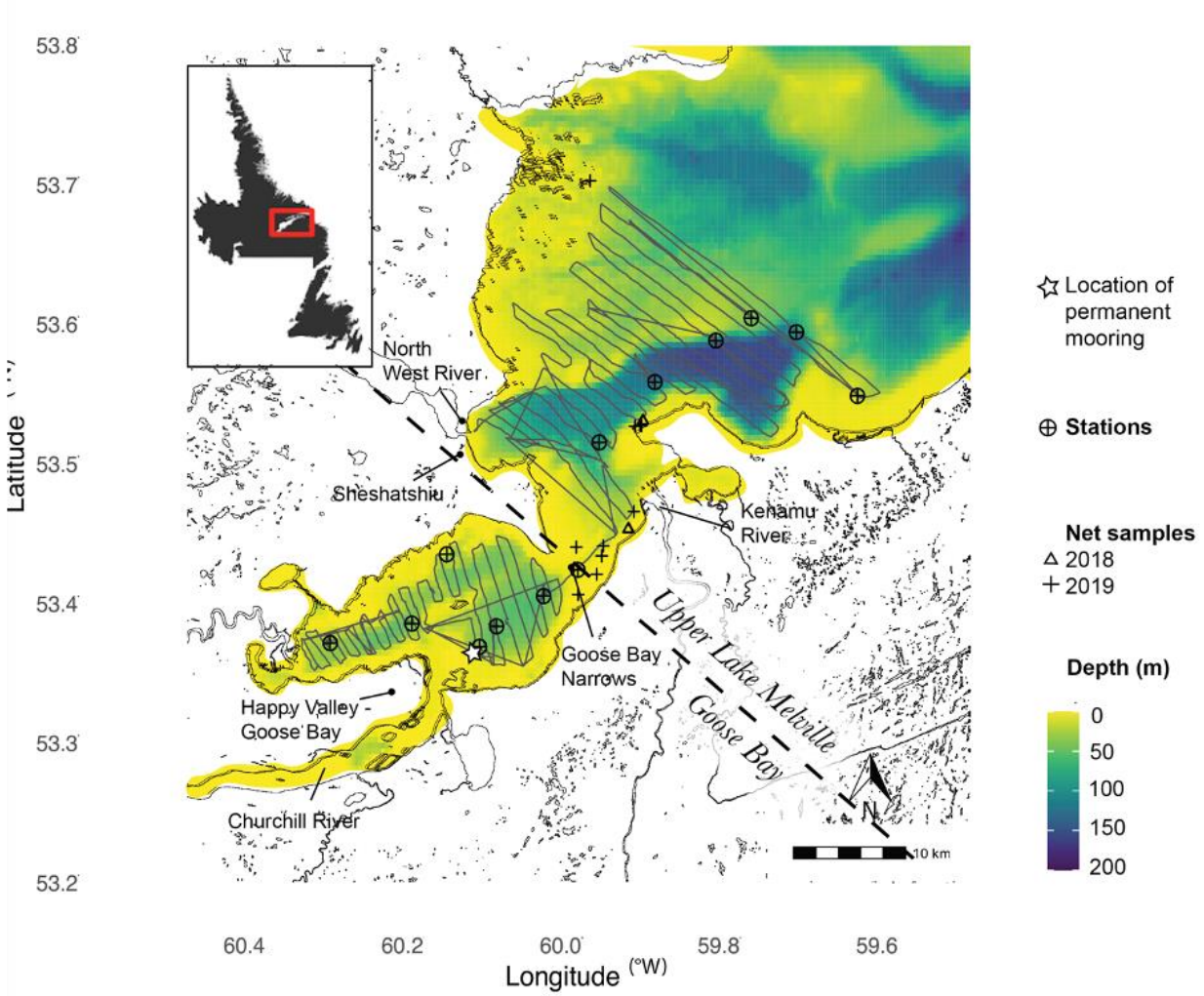

Figure 5. Bathymetric map of upper Lake Melville. The continuous gray line indicates the acoustic transect followed in summers 2018 and 2019. Environmental stations (dots) were samples in summer and winter. The locations of fyke and gill net sampling are denoted by triangles (2018) and crosses (2019). The star indicates the position of the long-term oceanographic mooring.

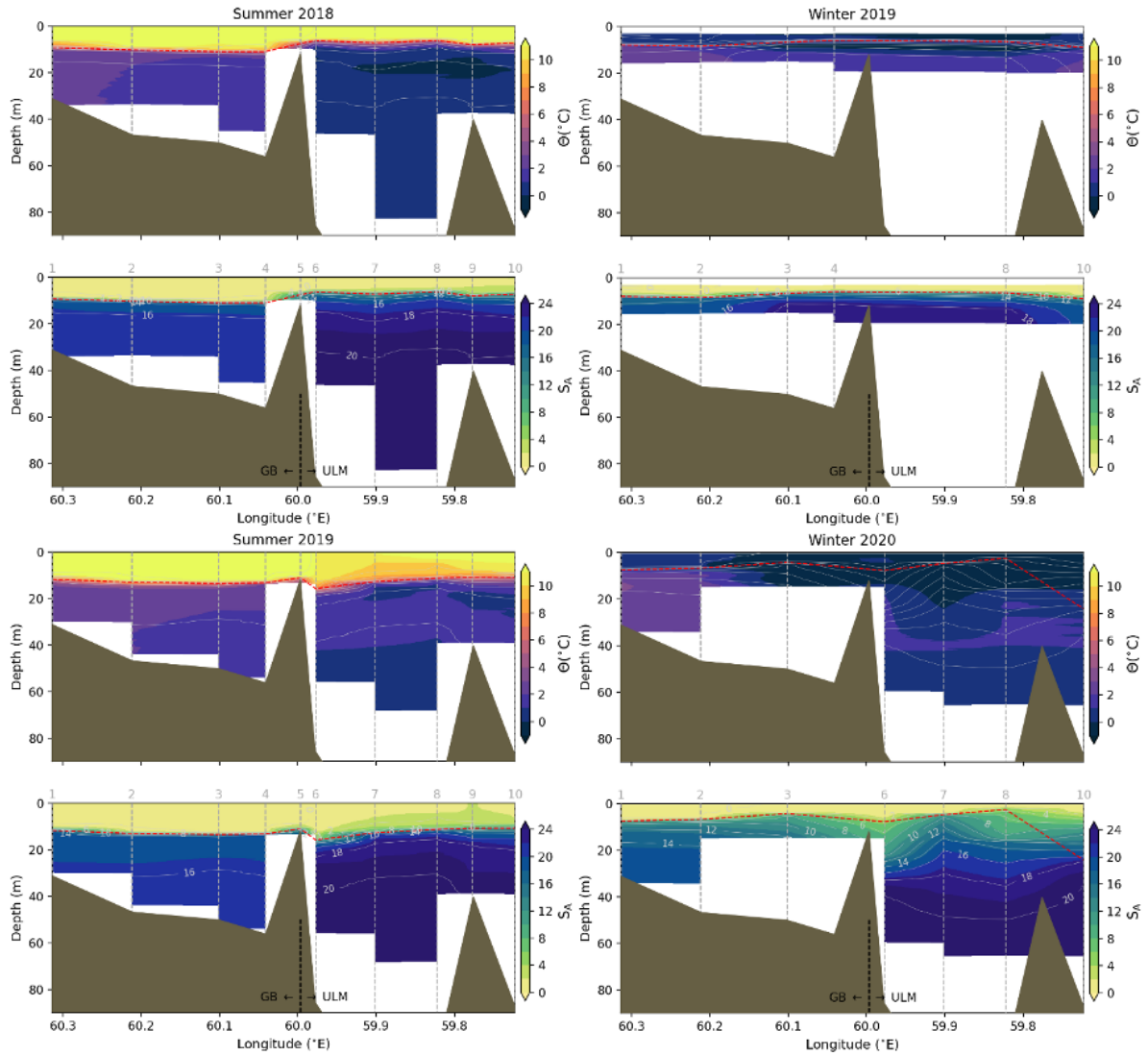

Figure 6. Section plots of conservative temperature (θ) and absolute salinity (SA) during summers 2018 and 2019 and winters 2019 and 2020 across Goose Bay (GB; west) and Upper Lake Melville (ULM; east). For each panel, the density anomaly referenced to surface (σ0; in kg m-3) is plotted as solid light gray lines identified in the salinity panels. The brown shaded polygon represents bottom drawn using the depth at each station determined with acoustics measurements. The grey dotted lines represent profile stations identified in the top of the salinity panels. White areas indicate the absence of data. The pycnocline is identified with a dashed-red lines. The separation between Goose Bay (GB) and Upper Melville Lake (ULM) occurs at the sill near station 5 and is identified in the salinity panel. Note that for winter 2019, a problem with the profiler prevented the presentation of data below ~20m.

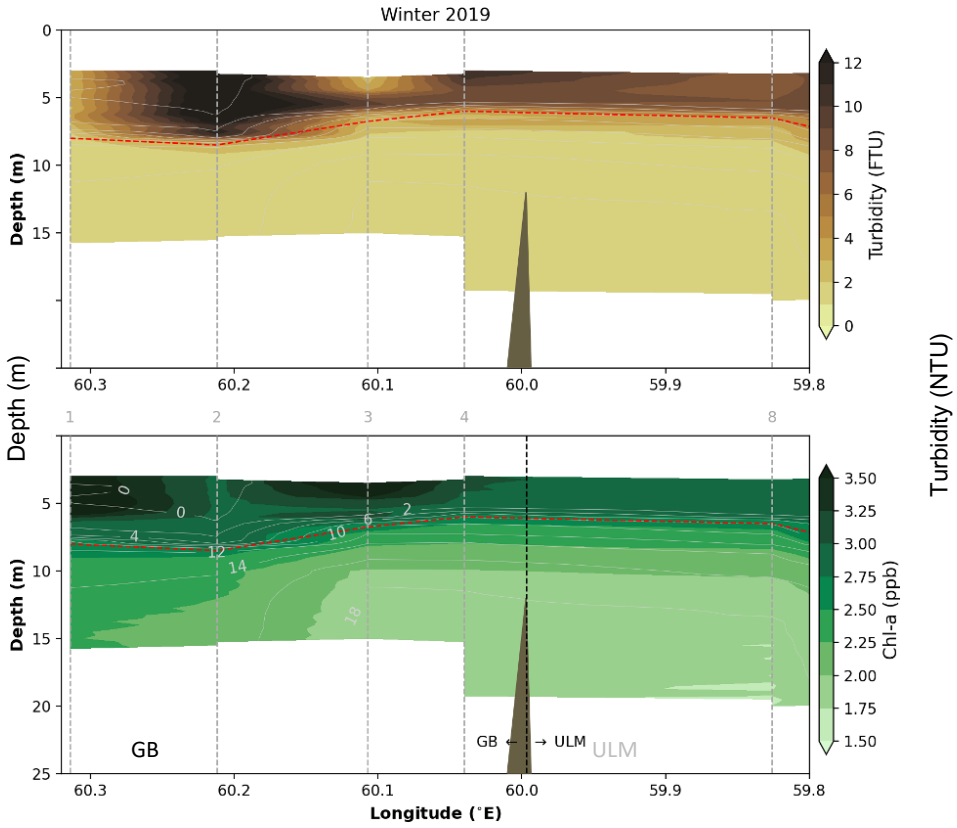

Figure 7. Turbidity (in Formazine Turbidity Unit; FTU) and chl-*a* (in part per billion; ppb) section plot for Goose Bay (GB) and Upper Lake Melville (ULM) during winter 2019. For each panel, the density anomaly referenced to surface (σ_0; in kg m^{-3}) is plotted as solid light gray lines identified in the chl-*a* panel. The vertical dashed lines indicate the location of the stations. The sill between GB and ULM is identified in brown.

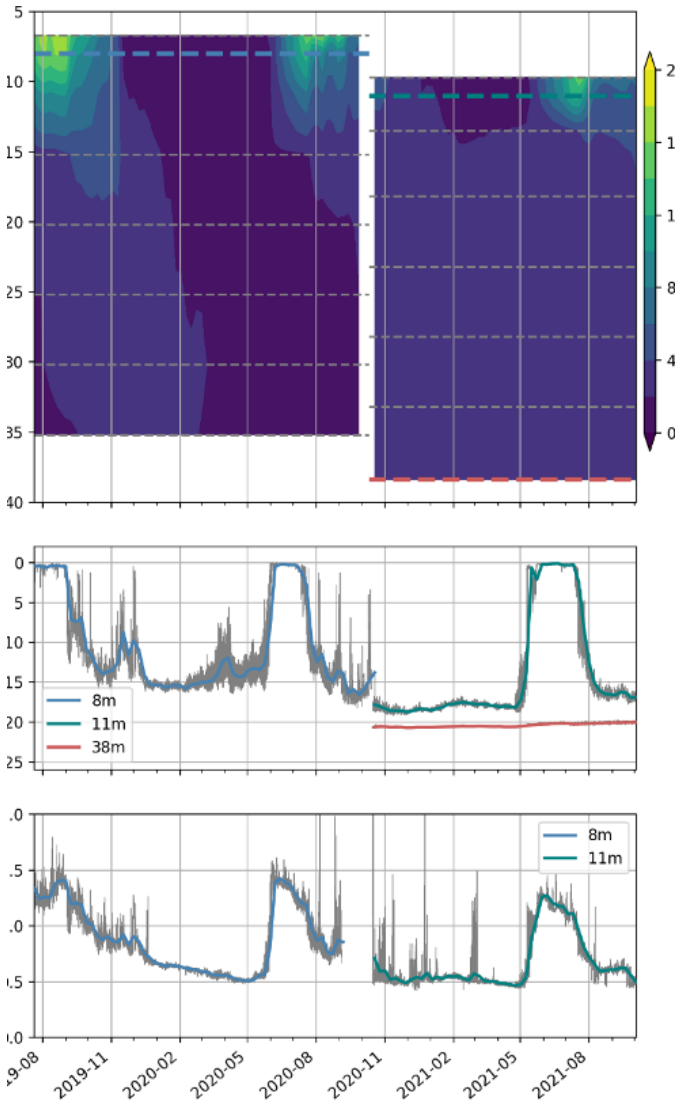

Figure 8. Temperature contours at the mooring location from two deployments (2019-07-15 to 2020-10-14 and 2020-10-13 to 2021-10-04), from 6 TidbiTs temperature sensors (position identified with dashed-gray lines), one RBR CTD located at 8m during the first deployment (dashed-blue line) and 38.4m during the second deployment (dashed-red line) and one Seabird CTD located at 11m during the second deployment (dashed-green line). Note that during the second deployment, the mooring release got tangled bringing all instruments down by about 3 m from their targeted depth.

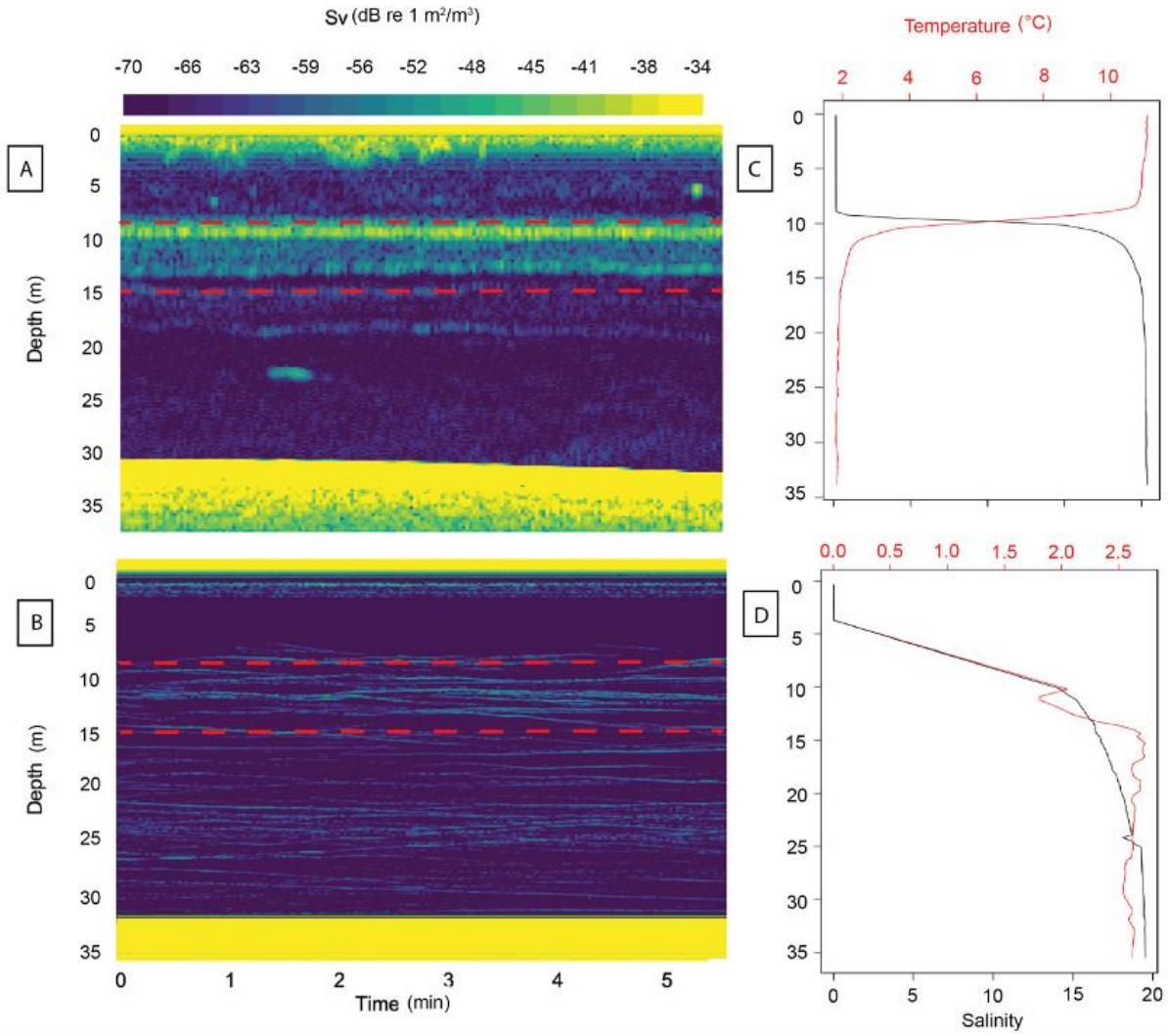

Figure 9. Examples of raw SV echograms at 38 kHz at station 2 during A) summer 2018 as measured with a hull mounted Simrad EK60; and B) winter 2019 as measured with a Simrad Wideband Autonomous Transceiver (WBAT). The dashed red lines indicate the sound scattering layer, which in this case was located between 9 and 15 m. Corresponding temperature (red) and salinity (black) profiles for station 2 in C) summer 2018 and D) winter 2019.

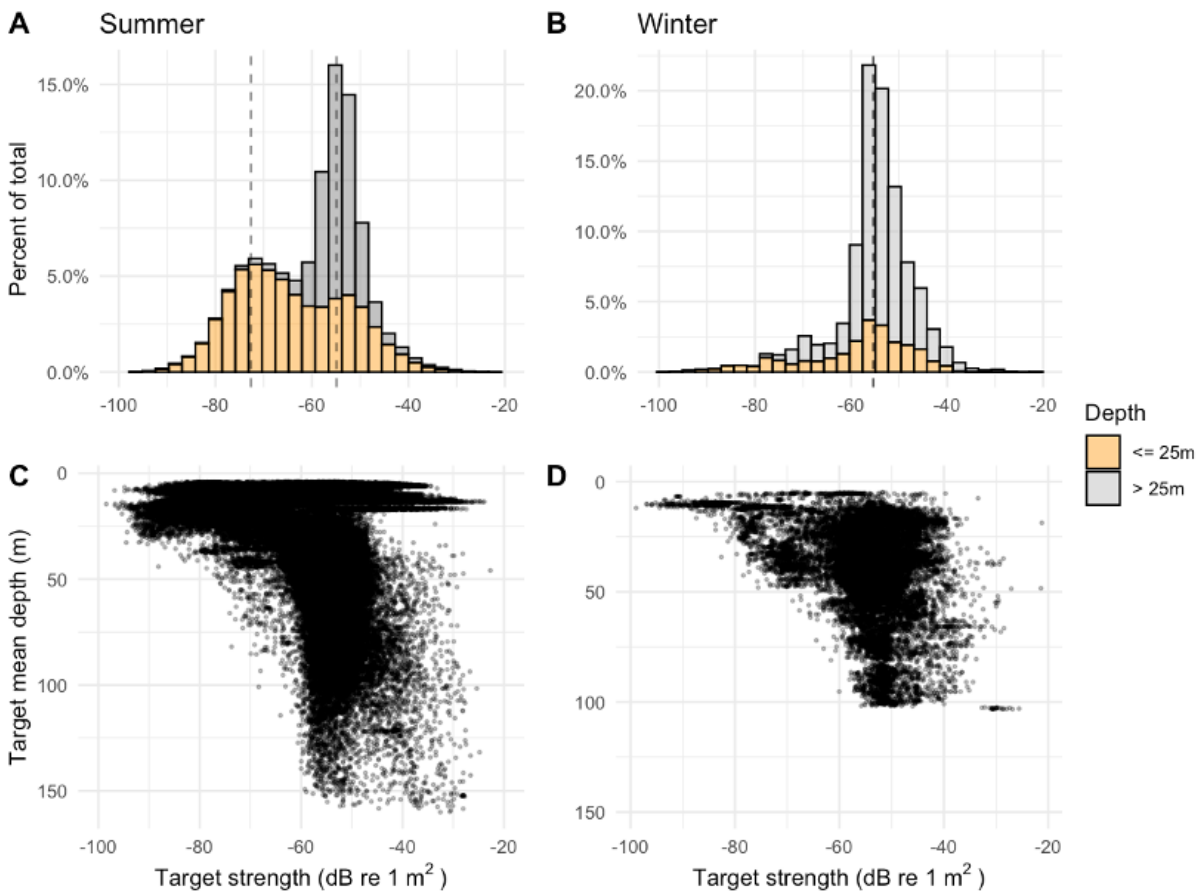

Figure 10. Percentage of total Target Strengths (TS) at 38 kHz for A) pooled summer data (2018-2019; n=122,924); and B) pooled winter data (2019-2020; n=18,175) at depth □25 m (orange) and >25 m (gray). Average depth of each target and their corresponding TS for targets detected in C) summer and D) winter. The maximum range of the WBAT and portable echosounder in winter was set to only 100 m.

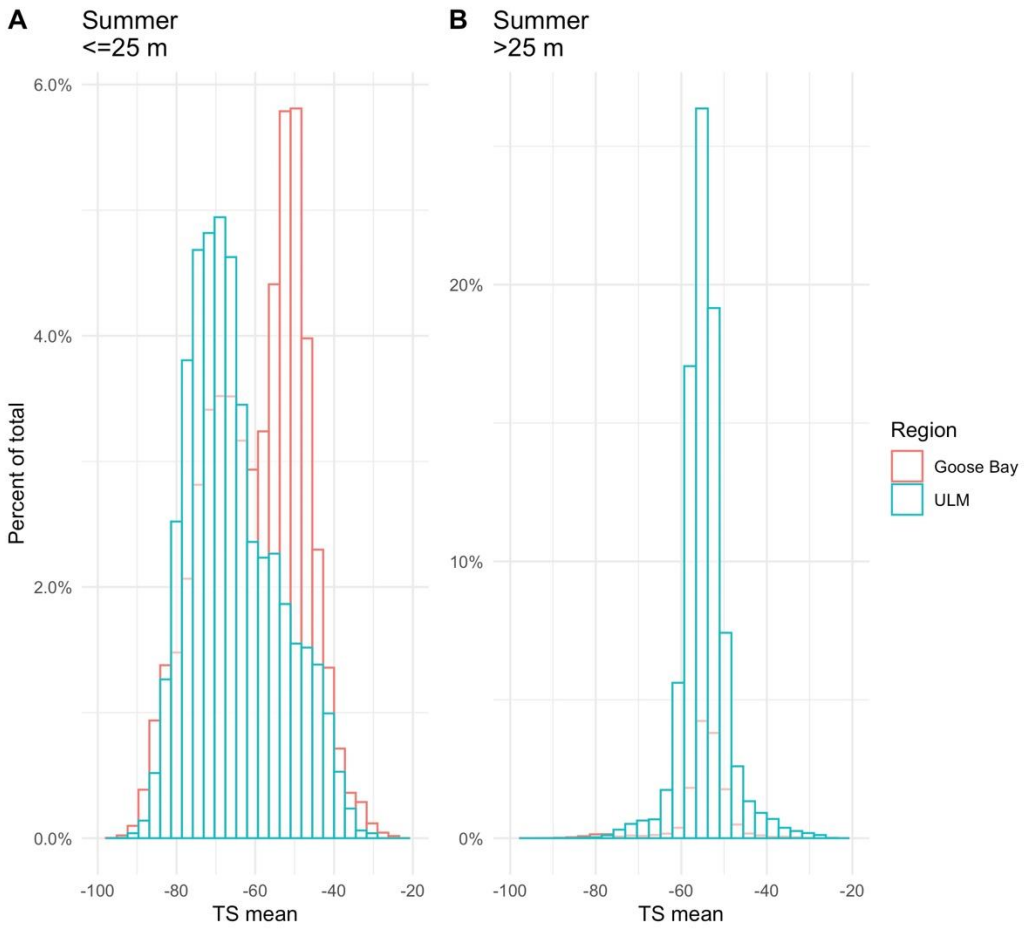

Figure 11. Percent total of Target Strength values of pooled results for summers 2018 and 2019, divided by regions (ULM (blue) and GB (red)). Showing TS distributions, A) ≤ 25 m and B) in depths greater than 25 m.

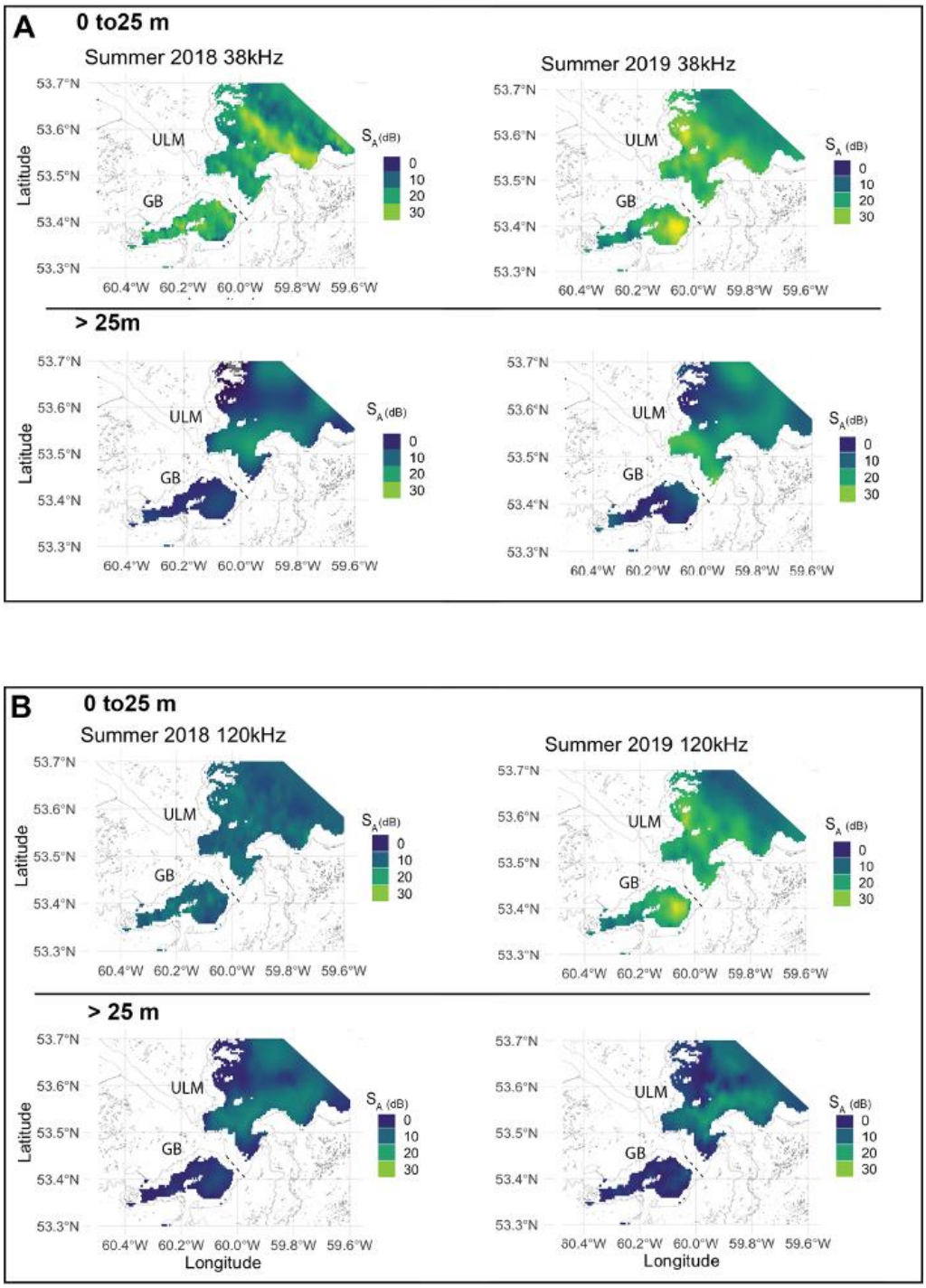

Figure 12. Kriged nautical area scattering strength (S_A in dB re $1m^2$ nmi^{-2}) at A) 38 kHz and B) 120 kHz above and below 25 m. The dashed line delineates Goose Bay (GB) and upper Lake Melville (ULM).

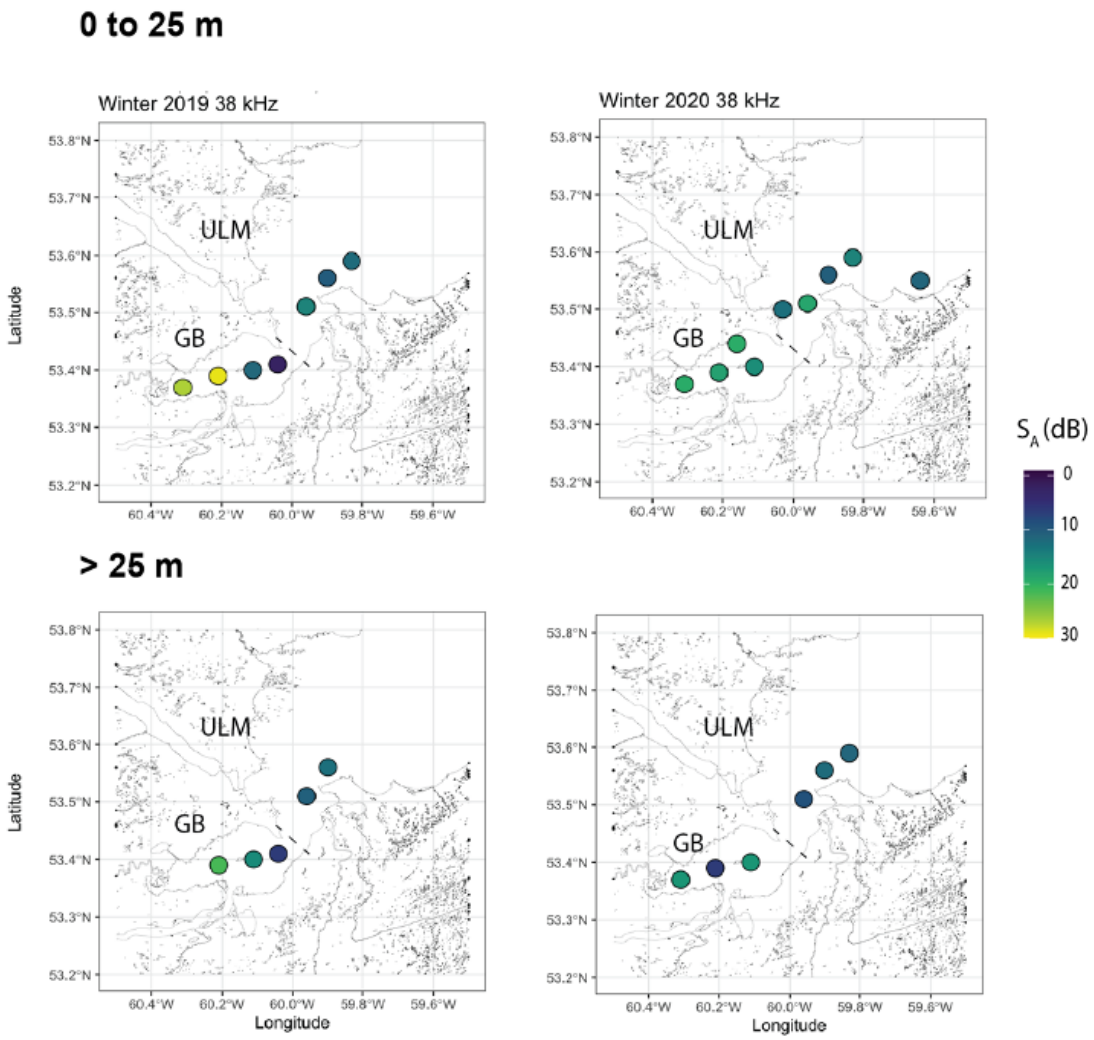

Figure 13. Nautical area scattering strength (S_A in dB re $1m^2$ nmi^{-2}) at 38 kHz above and below 25m. The dashed line delineates Goose Bay (GB) and upper Lake Melville (ULM).

Tables

Table 1. Average seasonal pycnocline depth, temperature, and salinity above (surface layer) and below (bottom waters) the pycnocline in Goose Bay and Upper Lake Melville. The information is divided into year 1 (2018-2019) and year 2 (2019-2020) of the survey. Standard variation is indicated.

		Goose Bay		Upper Lake Melville	
		Summer	Winter	Summer	Winter
Pycnocline depth (m)	Year 1	10.4 (± 0.8)	7 (± 1)	6.4 (± 0.6)	11 (± 8)
	Year 2	12.6 (± 0.8)	8 (± 2)	13(± 3)	15 (± 10)
Temp. surface layer (˚C)	Year 1	10.4 (± 0.4)	0.03 (± 0.04)	11.8 (± 0.1)	-0.08 (± 0.03)
	Year 2	12.0 (± 0.5)	0.100 (± 0.1)	9.35 (± 0.6)	-0.3 (± 0.2)
Salinity surface layer	Year 1	1.00 (±0.8)	2 (± 2)	2.1 (± 0.7)	10 (± 6)
	Year 2	0.8 (± 0.9)	1.80 (± 0.7)	3(± 2)	4 (± 2)
Temperature bottom waters (˚C)	Year 1	2.0 (± 0.2)	1.6 (± 0.7)	0.6 (± 0.1)	0.9 (± 0.2)
	Year 2	2.2 (± 0.2)	2.3 (± 0.7)	1.10 (± 0.4)	0.7 (± 0.2)
Salinity bottom waters	Year 1	19.9 (± 0.3)	19 (± 2)	24 (± 1)	18 (± 6)
	Year 2	19.7 (± 0.2)	18.2 (± 0.4)	24 (± 1)	23 (± 2)

Table 2. Mean abundance and biomass in fyke and gill nets

Species	2018			2019		
	Abundance CPUE (freq/hr)	Biomass CPUE (kg/hr)	Average length (mm)	Abundance CPUE (freq/hr)	Biomass CPUE (kg/hr)	Average length (mm)
White sucker	4.8 (n=77)	0.655	222 (± 23.0)	1.3 (n=21)	0.174	215 (± 29.0)
Longnose sucker	3.7 (n=59)	0.285	183 (± 44.0)	4.3 (n=68)	0.387	192 (± 46.0)
Brook trout	3.0 (n=47)	0.922	298 (± 52.0)	0.6 (n=10)	0.051	185 (± 45.0)
Tomcod	2.6 (n=41)	0.0330	112 (± 29.0)	2.4 (n=39)	0.0360	100 (± 49.0)
Lake chub	2.4 (n=39)	0.0240	93.0 (± 13.0)	1.9 (n=30)	0.0150	86 (± 18)
Rainbow smelt	0.6 (n=9)	0.207	162 (± 42.0)	1.2 (n=20)	0.0430	157 (± 38.0)
Threespine stickleback	0.1 (n=2)	0.000	54 (± 8.0)	1.4 (n=22)	0.00200	50 (± 3.0)
Winter flounder	0.1 (n=1)	0.00700	192	0	0	NA
Sculpin	0	0	NA	0.1 (n=1)	0.000	85

Table 3. Shannon-Weiner diversity Index (H) by region and year calculated from catches in gill and fyke nets deployed in shallow water (<2m).

Region (n = number of stations)	Year	H (Diversity Index)
ULM (n=6)	2018	1.72
ULM (n=9)	2019	1.66
GB (n=1)	2019	1.20

Table 4 Environmental DNA hits above and below the pycnocline in Upper Lake Melville and Goose Bay divided based on species habitat (blue = Marine, grey = Freshwater, green = Anadromous).

Habitat	Group	Genus	Species	Common Name	Upper Lake Melville		Goose Bay	
					#of sequences above pycnocline	# of sequences below pycnocline	# of sequences above pycnocline	#of sequences below pycnocline
Marine	Gadidae	*Melanogrammus*	*aeglefinus*	Haddock	77	723	1494	187
	Salmonidae	*Salvelinus*	*alpinus*	Arctic char	231	710	NA	NA
	Ammodytidae	*Ammodytes*	*americanus*	American sand eel	285	4489	NA	NA
	Hemitripteridae	*Hemitripterus*	*americanus*	Sea raven	170	NA	NA	NA
	Ammodytidae	*Ammodytes*	*dubius, hexapterus*	Northern sandlance, Pacific sandlance	214	NA	NA	NA
	Cottidae	*Cottus*	*asper*	Prickly sculpins	287	134	100	NA
	Cottidae	*Myoxocephalus*	*scorpius, thompsoni*	Shorthorn sculpin, Deepwater sculpin	9105	1808	140	166
	Agonidae	*Leptagonus*	*decagonus*	Atlantic poacher	NA	1494	NA	NA
	Ammodytidae	*Ammodytes*	*dubius*	Northern sandlance	NA	51	NA	NA
	Gadidae	Spp.	Arctogadus *glacialis,* Gadus *morhua, Gadus ogac*	Arctic cod, Atlantic cod, Greenland cod	NA	416	185	146
	Gadidae	*Gadus*	*morhua, ogac*	Atlantic cod, Greenland cod	14751	148308	62074	35294
	Gadidae	Spp.	Gadus *ogac, Melanogrammus aeglefinus*	Greenland cod, Haddock	NA	103	NA	NA
	Gadidae	Spp.	*Gadus morhua, Gadus ogac, Melanogrammus aeglefinus*	Atlantic cod, Greenland cod, Haddock	67	896	299	226
	Pholidae	*Pholis*	*gunnellus*	Rock gunnel	3427	7312	NA	NA
	Clupeidae	*Clupea*	*harengus*	Herring	NA	204	1330	NA
	Ammodytidae	*Ammodytes*	*hexapterus*	Pacific sandlance	23425	38510	NA	NA
	Stichaeidae	*Lumpenus*	*lampretaeformis*	Snakeblenny	NA	1617	NA	1001
	Zoarcidae	*Lycodes*	*lavalaei*	Newfoundland eelpout	NA	1277	4787	5040
	Liparidae	*Liparis*	*fabricii, inquilinus*	Gelatinous snailfish, Inquiline snailfish	1714	15893	NA	NA
	Cyclopteridae	*Cyclopterus*	*lumpus*	Lumpfish	8177	NA	NA	NA
	Stichaeidae	*Leptoclinus*	*maculatus*	Daubed shanny	363	NA	NA	NA
	Sebastidae	*Sebastes*	*mentella*	Atlantic redfish	NA	NA	667	NA
	Gadidae	*Gadus*	*morhua*	Atlantic cod	116	1362	11890	275

	Gadidae	*Gadus*	*ogac*	Greenland cod	97	996	433	261
	Pleuronectidae	Spp.	*Hippoglossoides platessoides, Hippoglossus hippoglossus*	American plaice, Halibut	NA	NA	224	NA
	Pleuronectidae	Spp.	*Hippoglossoides platessoides, Hippoglossus hippoglossus, Pseudopleuronectes americanus*	American plaice, Halibut, Winter flounder	NA	NA	NA	1616
	Pleuronectidae	Spp.	*Hippoglossoides platessoides, Limanda ferruginea, Pseudopleuronectes americanus*	American plaice, Common dab, Winter flounder	NA	NA	NA	864
	Pleuronectidae	Spp.	*Hippoglossoides platessoides, Limanda ferruginea*	American plaice, Common dab	NA	NA	122	NA
	Pleuronectidae	spp.	*Hippoglossoides platessoides, Pseudopleuronectes americanus*	American plaice, Winter fllounder	10860	9128	92082	466529
	Pleuronectidae	*Hippoglossus*	*hippoglossus*	Halibut	NA	NA	989	62
	Pleuronectidae	*Limanda*	*ferruginea*	Common dab	310	297	381	3359
	Stichaeidae	*Eumesogrammus*	*praecisus*	Fourline snakeblenny	65	NA	NA	NA
	Gadidae	*Boreogadus*	*saida*	Polar cod	24441	10597	4017	1975
	Stichaeidae	Spp.	*Eumesogrammus praecisus , Leptoclinus maculatus*	Fourline snakeblenny, Daubed shanny	1478	NA	638	NA
	Cottidae	*Gymnocanthus*	*tricuspis*	Arctic staghorn sculpin	1953	NA	1678	NA
	Osmeridae	*Mallotus*	*villosus*	Capelin	16300	7455	20097	11384
	Zoarcidae	*Gymnelus*	*viridis*	Fish doctor	NA	NA	2301	NA
Freshwater	Cyprinidae	*Rhinichthys*	*cataractae*	Longnose dace	57349	41598	21271	1269
	Catostomidae	*Catostomus*	*catostomus*	Longnose sucker	52834	63485	69073	NA
	Catostomidae	*Catostomus*	*commersoni*	White sucker	39636	39181	52209	1171
	Cottidae	*Cottus*	*bairdii, cognatus*	Mottled scuplin, slimy sculpin	40557	53906	61094	987
	Salmonidae	Prosopium	*cylindraceum*	Round whitefish	227	237	161	NA
	Lotidae	*Lota*	*lota*	Burbot	6652	15777	21259	NA

	Esocidae	*Esox*	*lucius*	Northern pike	2587	3476	7388	NA
	Cyprinidae	*Margariscus*	*margarita*	Allegheny pearl dace	1135	NA	129	NA
	Salmonidae	*Salvelinus*	*namaycush*	Lake trout	365	NA	NA	NA
	Cyprinidae	*Couesius*	*plumbeus*	Lake chub	32909	36930	27299	NA
	Salmonidae	*Prosopium*	*cylindraceum, williamsoni*	Round whitefish, Mountain whitefish	2230	3536	1761	NA
	Salmonidae	*Salvelinus*	*fontinalis*	Brook trout	15436	9582	12529	NA
Anadromous	Gasterosteidae	*Gasterosteus*	*aculeatus*	Three-spined stickleback	35298	48074	23335	3225
	Osmeridae	*Osmerus*	*mordax*	Rainbow smelt	3183	861	6091	NA
	Gasterosteidae	*Pungitius*	*pungitius*	Ninespine stickleback	898	798	NA	643
	Salmonidae	*Salmo*	*salar*	Atlantic salmon	10612	5967	14016	624
	Salmonidae	Spp.	Coregonus *autumnalis,* Coregonus *lavaretus,* Stenodus *leucichthys*	Arctic cisco, Common whitefish, Sheefish	1084	1240	1627	NA
	Merlucciidae	*Microgadus*	*tomcod*	Atlantic tomcod	19444	43522	8469	12541
	Casterosteidae	*Gasterosteus*	*wheatlandi*	Blackspotted stickleback	1127	711	NA	NA

Appendix

Supplementary material

Supplementary Table 1. Details of all sampling stations.

Station	Latitude (˚N)	Longitude (˚W)	Summer 2018	Winter 2019	Summer 2019	Winter 2020
1	53° 22.353'	60° 18.781'	X	X	X	X
2	53° 23.184'	60° 12.550'	X	X	X	X
3	53° 23.070'	60° 6.089'	X	X	X	X
3’	53° 26.185'	60° 9.878'				X (WBAT only)
4	53° 24.384'	60° 2.501'	X	X	X	
5	53° 25.517'	59° 59.897'	X		X	
6	53° 31.008'	59° 58.258'	X	X (WBAT only)	X	X
7	53° 33.606'	59° 54.099'	X		X	X
8	53° 35.406'	59° 49.348'	X	X	X	X
9	53° 36.375'	59° 46.650'	X		X	
10	53° 35.768'	59° 43.217'	X	X	X	X
11	53° 33.024'	59° 38.546'				X (WBAT only)
Mooring	53° 22.188'	60° 7.392'	X	X	X	X

Supplementary Table 2. Acoustic equipment settings and specifications for summer and winter surveys.

Season / Transducer	**Frequency**			
	38 kHz		200 kHz	
	Pulse length	3 dB beam angle	Pulse length	3 dB beam angle
Summer 2018 (EK60)	1.024	6.87°	-	-
Winter 2019 (WBAT)	1.024	18°	-	-
Summer 2019 (EK60)	1.024	7.07°	-	-
Winter 2020 (EK80 portable)	2.048	17.10°	2.048	16.90°

Supplementary Table 3a. Parameters of Echoview single-echo detection algorithm for split beam echosounders (method 2) for summer surveys. A threshold of -110 dB was used.

Parameters	**Values**
Compensated TS threshold (dB)	-110.0
Pulse length determination level (dB)	6.0
Minimum normalized pulse length	0.7
Maximum normalized pulse length	1.5
Beam compensation model	Simrad LOBE
Maximum beam compensation (dB)	4.0
Maximum standard deviation of minor-axis angles (°)	0.6
Maximum standard deviation of major-axis angles (°)	0.6

Supplementary Table 3b. Parameters of Echoview single-echo detection algorithm for wideband for winter surveys. A threshold of -110 dB was used.

Parameters	**Values**
Compensated TS threshold (dB)	-110.0
Pulse length determination level (dB)	6.0
Minimum normalized pulse length	0.5
Maximum normalized pulse length	1.5
Minimum target separation	0
Beam compensation model	Simrad LOBE
Maximum beam compensation (dB)	4.0
Maximum standard deviation of minor-axis angles (°)	0.6
Maximum standard deviation of major-axis angles (°)	0.6

Supplementary Table 4. Settings of Echoview fish tracking algorithm (fish tracks in Echoview) used to detect single targets. We tracked targets over 1 ping with no missed detection between pings.

Parameters	**Values**
Data	4D (range, angles and time)
Weights - Major axis	30
Weights - Minor axis	30
Weights - Range	40
Weights - TS	0
Weights - ping gap	0
Track acceptance – Min. number of single targets in a track	1
Track acceptance – Min. number of pings in track	1
Track acceptance – Max. gap between single targets (pings)	0